How does water yield respond to mountain pine beetle infestation in a semiarid forest?

Jianning Ren[1,3], Jennifer Adam[1], Jeffrey A. Hicke[2], Erin Hanan[3], Naomi Tague[4], Mingliang Liu[1], Crystal Kolden[5], John T. Abatzoglou[5]

[1] Department of Civil & Environmental Engineering, Washington State University, 99163, Pullman, USA

[2] Department of Geography, University of Idaho, 83844, Moscow, USA

[3] Department of Natural Resources and Environmental Sciences, University of Nevada, 89501, Reno, USA

[4] Bren School of Environmental Science & Management, University of California, 93106, Santa Barbara, USA

[5] Management of Complex Systems, University of California, 95344, Merced, USA

Correspondence: Jennifer Adam (jcadam@wsu.edu)

Key points:

- Mountain pine beetle (MPB)-caused tree mortality increases water yield in most wet years, and decreases in water yield mainly happen in dry years; therefore, interannual climate variability is an important driver of water yield response to beetle-caused tree mortality.
- A long-term (multi-decade) aridity index is a reliable indicator of water yield response to MPBs: in a dry year, decreases in water yield occur mainly in water-limited areas and the level of vegetation mortality only has minor effects; in wetter areas, decreases in water yield only occur at low vegetation mortality levels.
- Generally, in a dry year, low to medium MPB-caused vegetation mortality decreases water yield, and high mortality increases water yield; this response to mortality level is nonlinear and varies by location and year.

Graphical abstract

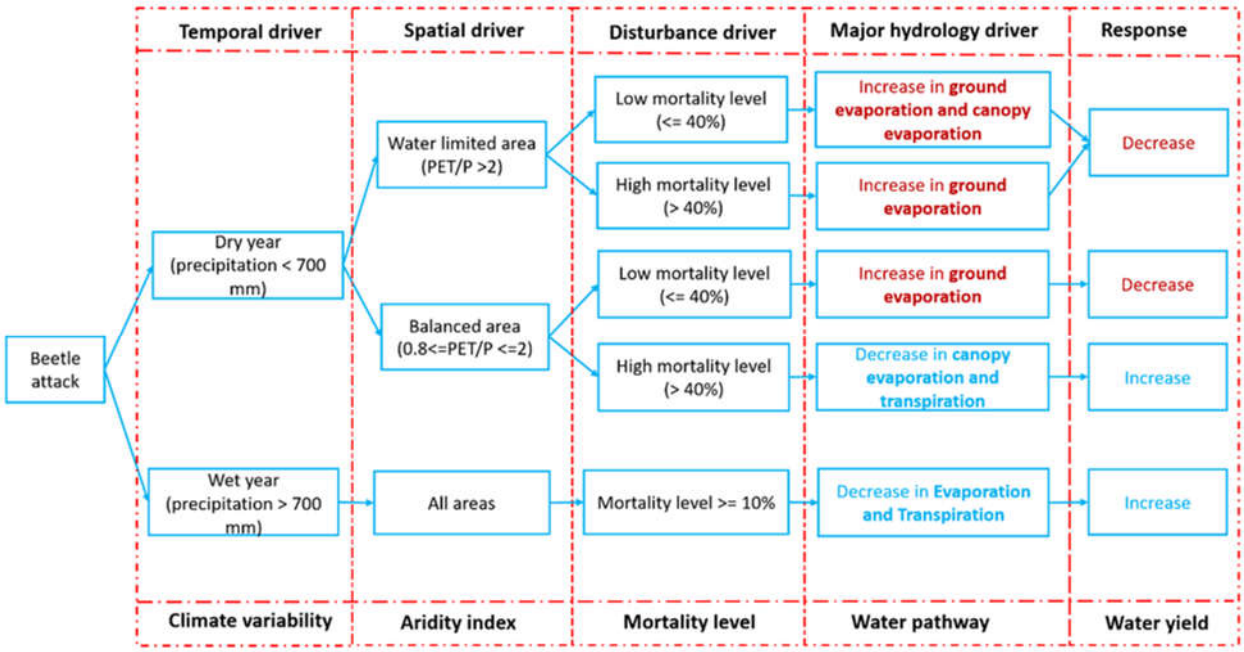

Abstract

Mountain pine beetle (MPB) outbreaks in the western United States result in widespread tree mortality, transforming forest structure within watersheds. While there is evidence that these changes can alter the timing and quantity of streamflow, there is substantial variation in both the magnitude and direction of hydrologic responses, and the climatic and environmental mechanisms driving this variation are not well understood. Herein, we coupled an eco-hydrologic model (RHESSys) with a beetle effects model and applied it to a semiarid watershed, Trail Creek, in the Bigwood River basin in central Idaho, USA, to examine how varying degrees of beetle-caused tree mortality influence water yield. Simulation results show that water yield during the first 15 years after beetle outbreak is controlled by interactions among interannual climate variability, the extent of vegetation mortality, and long-term aridity. During wet years, water yield after beetle outbreak increased with greater tree mortality; this was driven by mortality-caused decreases in evapotranspiration. During dry years, water yield decreased at low

to medium mortality but increased at high mortality. The mortality threshold for the direction of change was location-specific. The change in water yield also varied spatially along aridity gradients during dry years. In relatively wetter areas of the Trail Creek basin, post-outbreak water yield decreased at low mortality (driven by an increase in ground evaporation) and increased when vegetation mortality was greater than 40 percent (driven by a decrease in canopy evaporation and transpiration). In contrast, in more water-limited areas, water yield typically decreased after beetle outbreaks, regardless of mortality level (although the driving mechanisms varied). Our findings highlight the complexity and variability of hydrologic responses and suggest that long-term (i.e., multi-decadal mean) aridity can be a useful indicator for the direction of water yield changes after disturbance.

1 Introduction

In recent decades, mountain pine beetle (MPB) outbreaks in the Western U.S. and Canada have killed billions of coniferous trees (Bentz et al. 2010). Coniferous forests can provide essential ecosystem services, including water supply for local communities (Anderegg et al. 2013). Therefore, it is essential to understand how ecosystems and watersheds respond to beetle outbreaks and to identify the dominant processes that drive these responses (Bennett et al. 2018). A growing number of studies have qualitatively examined hydrologic responses to beetle outbreaks and disturbance; however, these studies have produced conflicting results (Adams et al. 2012; Goeking and Tarboton 2020). While some studies show increases in water yield following beetle outbreak (e.g., Bethlahmy 1974; Potts 1984; Livneh et al. 2015), many others show no change or even decreases (e.g., Guardiola-Claramonte et al. 2011; Biederman et al. 2014; Slinski et al. 2016). To determine which mechanisms control change in water yield following beetle outbreak, more quantitative approaches are needed.

Water yield is often thought to increase after vegetation is killed or removed by disturbances such as fire, thinning, and harvesting (Hubbart 2007; Robles et al. 2014; Chen et al. 2014; Buma and Livneh 2017; Wine et al. 2018). In the Rocky Mountain West, beetle outbreaks have increased water yield through multiple mechanisms. First, defoliation/needle loss can reduce plant transpiration, canopy evaporation, and canopy snow sublimation losses to the atmosphere (Montesi et al. 2004). Snow sublimation is an important process in snow-dominated forest systems. Beetle-caused decreases in total sublimation can increase water yield, especially since canopy sublimation is more sensitive to disturbances than ground snow sublimation (Frank et al. 2019). Increased canopy openings can also enable snow accumulation and allow more radiation to reach the ground surface, resulting in earlier and larger peak snowmelt events, which can in turn reduce soil moisture and therefore decrease summer evapotranspiration (ET).

Several studies have documented decreases in water yield following disturbances (e.g., mortality, fire, beetle outbreaks; Biederman et al. 2014; Bart et al. 2016; Slinski et al. 2016; Goeking and Tarboton 2020). For example, in the southwestern U.S., beetle outbreaks have decreased streamflow by opening forest canopies and increasing radiation to the understory and at the ground surface, which leads to increases in understory vegetation transpiration (Guardiola-Claramonte et al. 2011), soil evaporation, and therefore increases total ET (Bennett et al. 2018). Tree mortality or removal can reduce streamflow because surviving trees and/or understory vegetation compensates by using more water (Tague et al. 2019).

In a review of 78 studies, Goeking and Tarboton (2020) concluded that the decrease in water yield after tree-mortality mainly happens in semiarid regions. Previous studies also provide rule-of-thumb thresholds above which water yield will increase: at least 20 percent loss of vegetation cover and mean precipitation of 500 mm/year (Adams et al. 2012). However, many

watersheds in the western U.S. experience high interannual climate variability (Fyfe et al. 2017), and local environmental gradients (e.g., long-term aridity gradients) may strongly influence vegetation and hydrologic responses to disturbances such as beetle outbreaks, making such rules-of-thumb difficult to apply in practice (Winkler et al. 2014). Given the possibility of either increases or decreases in water yield following beetle outbreaks, modeling approaches are crucial for identifying the specific mechanisms that control these responses.

Our overarching goal was to identify mechanisms driving the direction of change in annual water yield after beetle outbreaks in semi-arid regions (note that in the following text, "water yield" refers to mean annual water yield). To accomplish this goal, we asked the following questions:

- **Q1:** What is the role of **interannual climate variability** in water yield response?
- **Q2:** What is the role of **mortality level** in water yield response?
- **Q3:** How does **long-term aridity** (defined as temporally averaged potential evapotranspiration relative to precipitation) modify these responses, and how do responses vary spatially within a watershed along aridity gradients?

We hypothesized that multiple ecohydrologic processes (e.g., snow accumulation and melt, evaporation, transpiration, drainage, and a range of forest structural and functional responses to beetles) could interactively influence how water yield responds to beetle outbreaks—however, in certain locations one or more processes may dominate. In addition, the dominant ecohydrologic processes may vary over space and time due to interannual climate variability (i.e., precipitation), vegetation mortality, and long-term aridity. In Section 2, we present a conceptual framework for identifying and depicting dominant hydrological processes through which forests respond to beetle infestation. We used this framework to interpret the modeling results. In

Section 3, we describe our mechanistic modeling approach, i.e., using the Regional Hydro-Ecological Simulation System (RHESSys), which can prescribe a range of vegetation mortality levels, capture the effects of landscape heterogeneity and the role of lateral soil moisture redistribution, and project ecosystem carbon and nitrogen dynamics, including post-disturbance plant recovery. In Sections 4 and 5, we then present modeling results that explore how multiple mechanisms influence water yield responses. This study can help inform management in beetle-affected watersheds by providing a tool for identifying locations that should be prioritized for mitigating flooding and erosion risk under different climate conditions.

2 Conceptual framework

2.1 Vegetation response to beetle outbreaks

Mountain pine beetles (MPB) introduce blue stain fungi into the xylem of attacked trees, which reduces water transport in plants and eventually shuts it off (Paine et al. 1997). During outbreaks, MPBs prefer to attack and kill larger host trees that have greater resources (e.g., carbon), while smaller diameter host trees and non-host vegetation (including the understory) remain unaffected (Edburg et al. 2012). After MBP outbreak, trees experience three phases (i.e., red, gray, and old) over time (Hicke et al. 2012). During the red phase, the trees' needles turn red. During the gray phase, there are no needles in the canopy. During old phase, killed trees have fallen, and understory vegetation and new seedlings experience rapid growth (Hicke et al. 2012; Mikkelson et al. 2013).

2.2 Hydrologic response to beetle outbreaks

Figure 1 describes the main processes that alter evapotranspiration to either decrease or increase water yield, depending on which processes dominate (Adams et al. 2012; Goeking and Tarboton 2020). During the red and gray phases, needles fall to the ground, and there is lower leaf area

141 index (LAI) and a more open canopy (Hicke et al. 2012). During these phases, changes in
142 canopy cover can interact with hydroclimatic conditions across a watershed to alter transpiration
143 and evaporation in a variety of ways.

144 Canopy mortality can reduce transpiration rates in infected trees, though in water-limited
145 environments, remaining trees may compensate to some extent by increasing transpiration
146 (Adams et al. 2012, Tague et al. 2019). More open canopies (i.e., following tree mortality)
147 intercept less precipitation than closed canopies, reducing canopy evaporation but potentially
148 increasing it from soil and litter layers (Montesi et al. 2004; Sexstone et al. 2018). Meanwhile,
149 open canopies can also increase the proportion of snow falling to the ground and, therefore,
150 increase snowpack accumulation. With more solar radiation reaching the ground, earlier and
151 larger peak snowmelt can also occur (Bennett et al. 2018). Generally, earlier snowmelt increases
152 water for spring streamflow and decreases water for summertime ET (Pomeroy et al. 2012).
153 However, once snags fall, reductions in longwave radiation can actually lead to later snowmelt
154 (Lundquist et al. 2013). An open canopy, combined with less competition for resources, such as
155 solar radiation and nutrients, can also promote understory vegetation growth, which may increase
156 understory transpiration (Biederman et al. 2014; Tague et al. 2019). In some riparian corridors,
157 the regreening of surviving vegetation and the compensatory response of remaining tissues could
158 diminish the reduction in ET caused by foliage fall, leading to no significant water yield response
159 to beetle-caused mortality (Snyder et al. 2012; Nagler et al. 2018). Therefore, whether water
160 yield increases or decreases following beetle outbreak ultimately depends on how these
161 processes interact.

Interannual variability in climate (e.g., dry versus wet years) can affect how hydrologic processes interact in forested watersheds (Winkler et al. 2014; Goeking and Tarboton 2020). For instance, during wet years, remaining plants are not water-limited, and reductions in plant transpiration due to beetle-caused mortality dominate over increases in soil evaporation or remaining plant transpiration, resulting in a higher water yield. In contrast, during dry years, plants are already under water stress and decreases in plant transpiration caused by tree mortality may be compensated by increasing soil evaporation and transpiration by remaining trees or understory vegetation, leading to declines in water yield. Moreover, these responses are also affected by land cover types (e.g., young versus old trees, different tree species, etc.), which is not currently well documented (Perry and Jones 2017; Morillas et al. 2017).

2.3 Review of modeling approaches

Many models, ranging from empirical and lumped to physically-based and fully-distributed, have been used to study hydrologic responses to disturbances. Goeking and Tarboton (2020) argue that only physically-based and fully-distributed models can capture how disturbances alter water yield because they represent fine-scale spatial heterogeneity and physical process that vary over space and time. Despite their advantages, many process-based models, such as the coupled CLM-ParFlow model (Mikkelson et al. 2013; Penn et al. 2016), the Distributed Hydrology Soil Vegetation Model (Livneh et al. 2015; Sun et al. 2018), and the Variable Infiltration Capacity Model (Bennett et al. 2018) also have some limitations. For example, 1) they may assume constant LAI after disturbances and static vegetation growth (e.g., VIC and DHSVM), 2) they may not include lateral flow to redistribute soil moisture (VIC), and 3) in some cases, the approach to represent the effects of beetle outbreaks may be too simplified (e.g., changing only LAI and conductance without considering two-way beetle-vegetation interactions in post-

185 disturbance biogeochemical and water cycling e.g., as in CLM-ParFlow). Thus, improving
186 current fully distributed process-based models to capture the coupled dynamics between
187 hydrology and vegetation at multiple scales is a critical step for projecting how beetle outbreaks
188 will affect water yield in semiarid systems (Goeking and Tarboton 2020). Here we use RHESSys
189 – Beetle model, which captures these processes.

190 **3 Model, data, and simulation experiment design**

191 3.1 Study area

192 Our study focused on the Trail Creek watershed, which is located in Blaine County between the
193 Sawtooth National Forest and the Salmon-Challis National Forest (43.44N, 114.19W; Fig. 2). It
194 is a 167-km^2 sub-catchment in the south part of Big Wood River basin and is within the
195 wildland-urban interface where residents are vulnerable to the flood and debris flows caused by
196 forest disturbances (Skinner 2013). Trail Creek has frequently experienced beetle outbreaks,
197 notably in 2004 and 2009, when beetles killed 7 and 19 km^2 of trees, respectively (Berner et al.
198 2017).

199 Trail Creek has cold, wet winters and warm, dry summers; mean annual precipitation is
200 approximately 978 mm, 60% of which falls as snow (Frenzel 1989). The soil is mostly
201 permeable coarse alluvium (Smith 1960). Elevations range from 1760 to 3478 m. Along this
202 elevation gradient, there are also strong vegetation and aridity gradients (Fig. 3). The northern
203 (higher elevation) portion of the basin is mesic and covered principally by evergreen forest,
204 containing Douglas-fir (*Pseudotsuga menziesii*), lodgepole pine (*Pinus contorta* var. *latifolia*),
205 subalpine fir (*Abies lasiocarpa*), and mixed shrub and herbaceous vegetation. The southern
206 (lower elevation) portion is xeric and covered by shrubs, grasses, and mixed herbaceous species,
207 including sagebrush, riparian species, and grasslands (Buhidar 2002).

In total, Trail creek contains 72 sub-basins and two of them (e.g., Fig. 3, sub-basin 412 and 416) are urban areas. When we classified this basin into different zones according to an aridity index, i.e., the ratio of 38-year average annual potential evapotranspiration (PET) to precipitation (P) (Section 3.4), two distinct hydrologic-vegetation cover types emerged: the northern and high elevation area is balanced (i.e., PET/P between 0.8 and 2) and evergreen tree coverage is more than 50%; the southern part is water-limited (i.e., PET/P > 2) and evergreen tree coverage is less than 30% (Figs. 2 and 3).

3.2 Model descriptions

3.2.1 Ecohydrologic model

The Regional Hydro-ecologic Simulation System (RHESSys; Tague and Band 2004) is a mechanistic model designed to simulate the effects of climate and land use change on ecosystem carbon and nitrogen cycling and hydrology. RHESSys fully couples hydrological processes (including streamflow, lateral flow, ET, and soil moisture, etc.), plant growth and vegetation dynamics (including photosynthesis, maintenance respiration, and mortality, etc.), and soil biogeochemical cycling (including soil organic matter decomposition, mineralization, nitrification, denitrification, and leaching, etc.). It has been widely tested and applied in several mountainous watersheds in western North America, including many in the Pacific and Inland Northwest (e.g., Tague and Band 2004; Garcia and Tague 2015; Hanan et al. 2017; 2018; 2021; Lin et al. 2019; Son and Tague 2019).

RHESSys represents a watershed using a hierarchical set of spatial units, including patches, zones, sub-basins, and the full basin, to simulate various hydrologic and biogeochemical processes occurring at these scales (Tague and Band 2004). The patch is the finest spatial scale at which vertical soil moisture and soil biogeochemistry are simulated. In every patch, there are

multiple canopy strata layers to simulate the biogeochemical processes related to plant growth and nutrient uptake. Meteorological forcing inputs (e.g., temperature, precipitation, humidity, wind speed, and solar radiation) are handled at the zone level, and spatially interpolated and downscaled for each patch based on elevation, slope, and aspect. Sub-basins are closed drainage areas entering both sides of a single stream reach (the water budget is closed in sub-basins). The largest spatial unit is the basin, which aggregates the streamflow from sub-basins (Tague and Band 2004; Hanan et al. 2018). In RHESSys, streamflow is the sum of overland flow and baseflow, and we consider streamflow as the ***water yield*** of each sub-basin.

RHESSys models vertical and lateral hydrologic fluxes, including canopy interception, plant transpiration, canopy evaporation/sublimation, snow accumulation, snowmelt and sublimation, soil evaporation, soil infiltration, and subsurface drainage. Canopy interception is based on the water-holding capacity of vegetation, which is also a function of plant area index (PAI). Both the canopy evaporation and transpiration are modeled using the standard Penman-Monteith equation (Monteith 1965). Snow accumulation is calculated from incoming precipitation and is assumed to fall evenly across each zone. Snowmelt is based on a quasi-energy budget approach accounting for radiation input, sensible and latent heat fluxes, and advection. Soil evaporation is constrained by both energy and atmospheric drivers, as well as a maximum exfiltration rate, which is controlled by soil moisture (Tague and Band 2004). Vertical drainage and lateral flow are a function of topography and soil hydraulic conductivity, which decays exponentially with depth (Tague and Band 2004; Hanan et al. 2018). Supplementary material section S1 contains a more detailed synopsis of the soil hydrologic model.

Vegetation carbon and nitrogen dynamics are calculated separately for each canopy layer within each patch, while soil and litter carbon and nitrogen cycling are simulated at the patch

level. Photosynthesis is calculated based on the Farquhar model, which considers the limitations of nitrogen, light, stomatal conductance (influenced by soil water availability), vapor pressure deficit, atmospheric CO_2 concentration, radiation, and air temperature (Farquhar and von Caemmerer 1982; Tague and Band 2004). Maintenance respiration is based on Ryan (1991), which computes respiration as a function of nitrogen concentration and air temperature. Growth respiration is calculated as a fixed ratio of new carbon allocation for each vegetation component (Ryan 1991; Tague and Band 2004). Net photosynthesis is allocated to leaves, stems, and roots at daily steps based on the Dickinson partitioning method, which varies with each plant development stage (Dickinson et al. 1998). LAI is estimated from leaf carbon and specific leaf area for each vegetation type. The soil and litter carbon and nitrogen cycling (heterotrophic respiration, mineralization, nitrification, and denitrification, etc.) are modified from the BIOME_BGC and CENTURY-NGAS models (White and Running 1994; Parton et al. 1996; Tague and Band 2004). A detailed description of RHESSys model algorithms can be found in Tague and Band (2004).

3.2.2 Beetle effects model

Edburg et al. (2012) designed and developed a model of MPB effects on carbon and nitrogen dynamics for integration with the Community Land Model Version 4 (CLM4) (Lawrence et al. 2011, Fig. 4). Here we integrated this beetle effects model into RHESSys (Fig. 4). Beetles attack trees mainly during late summer, and needles will turn from green to red at the beginning of the following summer. We simplify this process with prescribed tree mortality on September 1 to represent beetle outbreak for a given year. The advantage of this integration is that RHESSys accounts for the lateral connectivity in water and nitrogen fluxes among patches which is not represented in CLM4 (Fan et al. 2019). Our approach differs from other hydrological models of

277 beetle effects (e.g., VIC, CLM-ParFlow, and DHSVM) because it includes dynamic changes in
278 plant carbon and nitrogen cycling caused by beetle attack, plant recovery, and their effects on
279 hydrological responses. Previous studies of hydrologic effects of beetle outbreaks have mainly
280 focused on consequences of changes in LAI and stomatal resistance during each phase of
281 mortality but have missed feedbacks between carbon and nitrogen dynamics, vegetation
282 recovery, and hydrology (Mikkelson et al. 2013; Livneh et al. 2015; Penn et al. 2016; Sun et al.
283 2018; Bennett et al. 2018).

284 To better represent the effects of beetle-caused tree mortality, we added a snag pool
285 (standing dead tree stems) and a dead foliage pool (representing the red needle phase) in
286 RHESSys (Fig. 4). All leaf biomass (including carbon and nitrogen) become part of dead foliage
287 pools. After one year, the dead foliage is transferred to litter pools at an exponential rate with a
288 half-life of two years (Hicke et al. 2012; Edburg et al. 2011; 2012). Similarly, stem carbon and
289 nitrogen are moved to the snag pool immediately after outbreak. After five years, carbon and
290 nitrogen in snags begin to move into the coarse woody debris (CWD) pool at an exponential
291 decay rate with a half-life of ten years (Edburg et al. 2011; 2012). After outbreak, the coarse root
292 pools that are killed move to the CWD and fine root pools move to litter pools. To simplify, we
293 assume a uniform mortality level for all evergreen patches across landscape. Due to the
294 limitation of land cover data, we cannot separate pine and fir in these evergreen patches.
295 However, this will not affect the interpretation of our results because we analyze them based on
296 mortality level and evergreen vegetation coverage rather than different species.

297 In the integrated model, the reduction of leaf carbon and nitrogen after beetle outbreak can
298 directly decrease LAI and canopy height, which consequently affects energy (i.e., longwave
299 radiation and the interception of shortwave radiation) and hydrologic (i.e., transpiration and

canopy interception) fluxes. The model calculates two types of LAI: ***Live LAI*** (i.e., only live leaf is included), and ***Total LAI*** (i.e., both live and dead leaves are included). Plant transpiration is a function of *Live LAI*, while other canopy properties, including interception and canopy evaporation, is a function of *Total LAI*. The calculation of canopy height includes living stems and the snag pool.

3.3 Input data

We used the US Geologic Survey (USGS) National Elevation Dataset (NED) at 10 m resolution to calculate the topographic properties of Trail Creek, including elevation, slope, aspect, basin boundaries, sub-basins, and patches. Using NED, we delineated 16705 100-m resolution patches within 72 sub-basins. We used the National Land Cover Database (NLCD) to identify five vegetation and land cover types, i.e., evergreen, grass/herbaceous, shrub, deciduous, and urban (Homer et al. 2015). We determined soil properties for each patch using the POLARIS database (probabilistic remapping of SSURGO; Chaney et al. 2016). Parameters for soil and vegetation were based on previous research and literature (White et al. 2000; Law et al. 2003; Ackerly 2004; Berner and Law 2016; Hanan et al. 2016; 2021).

Climate inputs for this study, including maximum and minimum temperatures, precipitation, relative humidity, radiation, and wind speed, were acquired from gridMET for years from 1980 to 2018. GridMET provides daily high-resolution (1/24 degree or ~4 km) gridded meteorological data (Abatzoglou 2013). It is a blended climate dataset that combines the temporal attributes of gauge-based precipitation data from NLDAS-2 (Mitchell et al. 2004) with the spatial attributes of gridded climate data from PRISM (Daly et al. 1994).

3.4 Simulation experiments

To quantify how water yield responds to beetle-caused mortality, we prescribed a beetle outbreak in September 1989, where the mortality level (%) was applied to all evergreen patches for each sub-basin. After beetle outbreak, red needles remained on the trees for one year before they started to fall (transferred to the litter pool) at an exponential rate with a half-life of two years. The snag pools remained as standing trees for five years and then began to fall and were added to the CWD pool which decays at an exponential rate with a half-life of ten years.

To address Q1 (i.e., the role of interannual variability), we compared water yield responses during a dry water year, 1994 (i.e., five years after beetle outbreak with an annual precipitation of 611 mm), to responses during a wet year, 1995 (i.e., six years after beetle outbreak with an annual precipitation of 1394 mm). This enabled us to estimate the role of interannual climate variability in driving changes in water yield following beetle attack. The dry year was selected from years that had precipitation below the 15^{th} percentile of annual precipitation data (1980 to 2018; Searcy 1959; see Fig. S1). During the early period after beetle outbreak (e.g., 1994 and 1995) the forest experienced large changes in vegetation canopy cover, plant transpiration, and soil moisture. We chose these two successive years because their canopy and vegetation status were similar in terms of fallen dead foliage and residual vegetation regrowth, which makes this comparison reasonable. However, it is possible that antecedent climate conditions may affect the following year's response. For example, soil moisture can be depleted during a drought year, affecting initial conditions the following year. Moreover, under drought conditions, less reactive nitrogen is taken up by the plants or leaching is reduced, so more nitrogen will be left for the following year. Therefore, the difference in water yield responses between 1994 and 1995 might be affected by not only by climate variations but also initial hydrologic and biogeochemical

conditions. To consider the time lag effect (antecedent conditions affecting the current year's response), we also analyzed other dry and wet years.

To address Q2 (i.e., the role of vegetation mortality), we prescribed a range of beetle-caused mortality levels (i.e., from 10% to 60% by a step of 10% in terms of a reduction in carbon, uniformly applied to all evergreen patches for each sub-basin) and a control run (no mortality). This enabled us to quantify how forest water yield responded to the level of vegetation mortality (for each sub-basin **vegetation mortality** is **evergreen mortality** multiplied by evergreen coverage of that basin). The differences in water yield between each mortality level and the control run represent the effects of beetle kill: a positive value means that mortality increased water yield, and vice versa.

We quantified the water budget for each sub-basin to examine which hydrological processes contribute to the water yield responses: water yield (Q), precipitation (P), canopy evaporation (E_{canopy}, canopy evaporation and snow sublimation), transpiration (T), ground evaporation (E_{ground}, includes bare soil evaporation, pond evaporation, and litter evaporation), snow sublimation (Sublim, ground), soil storage change (dS_{soil}/dt), litter storage change (dS_{litter}/dt), snowpack storage change ($dS_{snowpack}/dt$) and canopy storage change (dS_{canopy}/dt). We summarized these rate variables at an annual time step.

The storage components include soil, litter, and canopy. According to Eq. (1), if the storage increases, water yield decreases.

$$Q = P - E_{canopy} - E_{ground} - Sublim - T - d\left(S_{soil} + S_{litter} + S_{canopy} + S_{snowpack}\right)/dt \quad (1)$$

Q: Water yield (mm/year)

P: Precipitation (mm/year)

E_{canopy}: Canopy evaporation (including canopy snow sublimation, mm/year)

E_{ground}: Ground evaporation includes bare soil evaporation, pond evaporation, and litter evaporation (mm/year)

T: Transpiration (mm/year)

Sublim: Ground snow sublimation (mm/year)

$\boldsymbol{dS_{soil}/_{dt}}$: Change in soil water storage calculated at yearly interval (mm/year)

$\boldsymbol{dS_{litter}/_{dt}}$: Change in litter water storage calculated at yearly interval (mm/year)

$\boldsymbol{dS_{canopy}/_{dt}}$: Change in canopy water storage calculated at yearly interval (mm/year)

$\boldsymbol{dS_{snowpack}/_{dt}}$: change in snowpack water storage calculated at yearly interval (mm/year)

Calculating water balance differences between different mortality scenarios and control scenario results in Eq. (2) (Note that precipitation is a model input and is unaffected by mortality and so ΔP = 0).

$$\Delta Q = \Delta E_{canopy} + \Delta E_{ground} + \Delta Sublim + \Delta T + \Delta\left(\frac{d\left(S_{soil} + S_{litter} + S_{canopy} + S_{snowpack}\right)}{dt}\right) \quad (2)$$

To address Q3 (i.e., the role of long-term aridity), we calculated a long-term aridity index (PET/P, Fig. 3) across the basin and analyzed the relationship between long-term aridity index and hydrologic response. As mentioned earlier, the long-term aridity index is defined as the ratio of mean annual potential ET (PET) to annual precipitation (P), averaged over 38 years (water year 1980-2018) of historical meteorological data. Based on the long-term aridity index, we

384 classified our sub-basins into three types (i.e., water-limited, balanced, energy-limited; McVicar
385 et al. 2012; Table 1).

386 **4 Results**

387 4.1 Simulated vegetation response to beetle outbreak at basin-scale

388 4.1.1 Vegetation response to beetle outbreaks

389 Figure 5 shows the basin-scale vegetation response after beetle outbreak in 1989. *Live LAI*
390 dropped immediately after beetle outbreak, then gradually recovered to pre-outbreak levels
391 during following years (Fig. 5a). *Total LAI* (i.e., including dead foliage slightly increased during
392 the first ten years after beetle outbreak (1990 – 2000), which was due to the retention of dead
393 leaves in the canopy and the simultaneous growth of residual (unaffected) overstory and
394 understory vegetation (Fig. 5b). The dead foliage pool (Fig. 5c) remained in place for one year
395 and then began to fall to ground (converted to litter) exponentially with a half-life of two years,
396 and the snag pool (Fig. 5d) remained in place for five years and then began to fall to ground
397 (converted to CWD) exponentially with a half-life of ten years. These behaviors of the dead
398 foliage and snag pools are similar to Edburg et al. (2012), which demonstrates that the integrated
399 model is simulating expected vegetation dynamics following beetle outbreak.

400 4.1.2 Time series of hydrologic response to beetle outbreak

401 Figure 6 shows the changes in simulated water fluxes and soil moisture over the basin after
402 beetle outbreak with various evergreen mortality levels. During the first 15 years after beetle
403 outbreak, scenarios where the evergreen mortality level was larger than zero had higher basin-
404 scale water yield than the control scenario (where the evergreen mortality level was zero). This
405 was especially true during wet years; however, there was no significant increase during dry years
406 (i.e., 1992, 1994, 2001, and 2004; Fig. 6a). The year-to-year soil storage fluxes responded

407 strongly in the first two years after beetle outbreak, then stabilized to the pre-outbreak condition
408 (Fig. 6b). Note that year-to-year soil storage change is not the same as soil water storage. After
409 beetle outbreak, the soil held some portion of the water that was not taken up by plants, but this
410 was constrained by the soil water holding capacity. This phenomenon indicates that the soil has
411 some resilience to vegetation change.

412 Beetle outbreaks reduced transpiration during wet years but did not have significant effects
413 in dry years (Fig. 6c). This occurred because transpiration in dry years was water-limited and
414 was therefore much lower than the potential rate (more water was partitioned to evaporation;
415 similar to Biederman et al. 2014). Thus, killing more trees had little effect on stand scale
416 transpiration because remaining trees used any water released by the dead trees in dry years. On
417 the other hand, plant transpiration in wet years was close to the potential rate; therefore,
418 decreases in canopy cover reduced transpiration. There was no apparent effect of beetle outbreak
419 on snowmelt.

420 Snow sublimation played an essential role in driving the evaporation responses we
421 observed. In the Trail Creek watershed, snow sublimation accounted for around 50% of total
422 evaporation (not shown in the figure), and around 60% came from the canopy. Canopy
423 sublimation accounted for an even larger proportion of total sublimation during high snow years
424 (Fig. S7 d and Fig. S1). These results are similar to other western US forests where 50 to 60% of
425 total sublimation has been found to come from canopy sublimation, which is more sensitive to
426 beetle kill than ground snow sublimation (Molotch et al. 2007; Frank et al. 2019). We also found
427 that during the first three years after beetle outbreak, when dead foliage was still on the canopy,
428 canopy sublimation increases by approximately 6% due to an increase in *Total LAI* as new
429 needles grew and dead foliage remained on the canopy. This increased canopy snow interception

and subsequent sublimation (Fig. 5). However, when the dead foliage fell to the ground and snags began to fall, the canopy sublimation decreased by approximately 10% for the most severe mortality scenario (60% evergreen mortality) compared to the no-outbreak scenario. This occurred because canopy *Total LAI* decreased and there was less canopy interception (Fig. 5).

Ground snow sublimation was less sensitive to beetle-kill (Fig. S7b). In the first three years after beetle-kill (at 60% mortality), ground snow sublimation increased by approximately 7.5% due to an increase of aerodynamic conductance caused by higher understory canopy height. However, from 1993 to 2002, there was no obvious changes in ground snow sublimation after beetle outbreak. When all dead foliage and more than 50% of snags fell to the ground, ground snow sublimation decreased because snowmelt increased as the canopy opened (Fig. 5 and Fig. S7b). In general, for the 60% mortality scenario, the ground snow sublimation first increased by approximately 5% when dead foliage is still on the trees, then decreased by approximately 6% when the canopy is open.

The evaporation response was opposite in dry and wet years: evaporation increased in dry years, while it decreased in wet years (Fig. 6d). This phenomenon is caused by tradeoffs and interactions among multiple processes, as will be explained in more detail in the next section.

4.2 The role of spatial heterogeneity in water yield response

4.2.1 Spatial patterns of hydrologic response along long-term aridity gradient

4.2.1.1 Evaporation

Beetle outbreak had opposite effects on evaporation between a dry year and a wet year (Fig. 7). In the dry year, most sub-basins experienced higher evaporation for beetle outbreak scenarios than in the control scenario (Fig. 7a). This was the cumulative consequence of

452 decreased canopy evaporation and increased ground (soil, litter, pond) evaporation due to
453 decreases in LAI (caused by mortality). In the dry year, the latter effect (i.e., increased ground
454 evaporation) dominated over the former, leading to an overall increase in evaporation. When the
455 vegetation mortality level (calculated as *the percentage of evergreen patches in a sub-basin*
456 *multiplied by the mortality level of evergreen caused by beetles*) was higher than 20%, a few sub-
457 basins in the balanced (more mesic) area experienced a decrease in evaporation, indicating that
458 the effects of decreasing canopy evaporation outstripped the effects of increasing ground
459 evaporation. In the wet year, most of the sub-basins located in the balanced area (where canopy
460 evaporation decreases dominated) experienced decreases in evaporation. This decrease
461 responded linearly to the level of vegetation mortality (Fig. 7b). However, sub-basins located in
462 much drier regions (aridity >3.5) had relatively minimal responses to the level of vegetation
463 mortality levels and some of them even had slight increases in evaporation (where ground
464 evaporation increases are dominant due to drier long-term climate and lower canopy mortality
465 resulted from less evergreen coverage).

466 4.2.1.2 Transpiration

467 Beetle outbreak decreased transpiration in both dry and wet years, and with higher mortality
468 levels the decrease became larger (Fig. 8). However, during the dry year, the water-limited area
469 experienced less change than the balanced area; some sub-basins even showed slight increases.
470 This increase in the water-limited part of the basin occurred because after beetles kill some
471 overstory evergreen trees, the living trees and understory plants together can exhibit higher
472 transpiration rates in dry years (Tsamir et al. 2019). In the wet year, when most canopies reach
473 potential transpiration rates (less competition for water), beetle outbreaks can reduce
474 transpiration rates by decreasing *Live LAI*.

4.2.1.3 Total ET

In a dry year, the balanced and water-limited areas had opposite responses to mortality: the balanced area experienced a decrease in ET and the water-limited area experienced a slight increase (Fig. 9). In the balanced area, larger ET decreases occurred with higher mortality levels. However, increases in ET in water-limited regions were less sensitive to vegetation mortality level, even when mortality was high (>40%), ET still increased (Fig. 9a). During the wet year, most sub-basins experienced decreasing ET after beetle outbreak and the magnitude was larger with higher vegetation mortality. The different responses of ET were driven by different hydrologic responses (transpiration, ground evaporation, and canopy evaporation) competing with each other; this competition was influenced by climate conditions, mortality level, and spatial heterogeneity in long-term aridity.

4.2.1.4 Water yield

In the dry year (1994), beetle-caused vegetation mortality affected water yield (Fig. 10), but the responses differed between the balanced and water-limited areas. For the **balanced area**, most sub-basins showed slight decreases in water yield after beetle outbreak and no significant differences among low vegetation mortality level (<=40%, Fig. 10a). However, with increased mortality, more sub-basins showed increases in water yield, particularly with vegetation mortality higher than 40% (Fig. 10a). Moreover, the vegetation mortality threshold that changed the direction of water yield response was altered by long-term aridity, e.g., it was 40% for aridity 2.0 but 20% for aridity 1.0. For **the water-limited** area, water yield decreased and was independent from mortality level (Fig. 10a). In the wet year (1995), the water yield in most sub-basins increased after beetle outbreak, and the balanced area increased more significantly than the water-limited area. Furthermore, in the balanced area, higher mortality levels caused larger

498 increases in water yield which responded more linearly (Fig. 10b). In summary, for a wet year,
499 increases in water yield occurred for most sub-basins, driven by a decrease in ET. However,
500 during dry years, the water yield and ET responses were spatially heterogeneous, and the
501 competing changes in evaporation and transpiration changed the direction and magnitude of ET
502 and thus water yield response. The competing effect among different hydrologic fluxes for a dry
503 year is explored in more detail in the next section.

504 4.2.2 Water budgets to understand decreasing water yield in the dry year
505 We analyzed the fluxes in greater detail in a dry year (1994) to understand the response of
506 hydrologic fluxes and resulting water yield. Based on Eq. (2), we identified four hydrological
507 fluxes that can potentially affect water yield: canopy evaporation (canopy evaporation and
508 canopy snow sublimation), ground evaporation (bare soil evaporation, ground snow sublimation,
509 litter evaporation, pond evaporation), plant transpiration, and year-to-year storage change (soil,
510 canopy, litter, snowpack). These three storage terms (canopy, litter, snowpack) were considered
511 together with soil storage since their contribution was minor in comparison with other fluxes.
512 Figure 11 summarized different combinations of these four dominate processes during the dry
513 year (1994) based on their directions (increase or decrease in water yield) after beetle outbreak.
514 In total, fourteen combinations of changes in these fluxes (referred to as “response types”) were
515 found. Five of them resulted in an increase in water yield, and the others resulted in a decrease.

516 Water yield responses caused by the competition of different hydrologic fluxes showed
517 different patterns across the aridity gradient (Figs. 3&10). For the balanced area (upper part of
518 the basin), with low evergreen mortality (<=30%), the major response types were D1 and D2, in
519 which the increase in ground evaporation dominated over the decrease in transpiration and
520 canopy evaporation (Fig. 11a, b, and c). However, with higher evergreen mortality (>30%), the

major response type became W2, where the increase in ground evaporation did not exceed the decrease in canopy evaporation and transpiration (Fig. 11e, f, and g). This indicates that, in a dry year, when more evergreen stands are killed, the increase in ground evaporation reaches a limit while transpiration and canopy evaporation continue to decrease with decreasing LAI. The increase in ground evaporation was triggered either by decreased *Total LAI* and open canopy, which allowed more solar radiation penetration to the ground for evaporation (Fig. S5c), or less transpiration from plants, which left more water available to evaporate (Fig. 8a). The decrease in plant transpiration and canopy evaporation was driven by a lower *Live LAI* and a lower *Total LAI*, respectively (Fig. S5 a&c and Fig. 8a).

The decrease in water yield in the water-limited area (i.e., the lower part of the basin) was driven by differences in how competing hydrologic responses interacted under different levels of mortality levels. When evergreen stand mortality level was low (<=30%), the response types were D5 and D7, in which the increase in ground and canopy evaporation dominated over the decrease of transpiration (Fig. 11a, b, and c). However, with high evergreen stand mortality (>30%), the response types became D1 and D2 (Fig. 11e, f, and g), in which the canopy evaporation changed from an increase to a decrease that was driven by a decrease in *Total LAI* (Fig. S5c). When mortality was low, the increases in growth from residual plants and understory outstripped the litter fall of dead foliage; thus, *Total LAI* increased, and vice versa when mortality was high.

5 Discussion

5.1 Role of interannual climate variability

During the first 15 years after beetle attack, various hydrologic processes opposed and/or reinforced one another to either increase or decrease water yield: a decrease in *Live LAI* can

reduce transpiration, while a decrease in *Total LAI* can enhance ground evaporation but diminish canopy evaporation (Montesi et al. 2004; Tsamir et al. 2019). Interannual climate variability plays an important role in determining which of these competing effects dominate and, therefore, drove the direction of water yield response to beetle outbreak (Winkler et al. 2014; Goeking and Tarboton 2020). Our results show that mainly decreases in water yield occurred in dry years, while in wet years water yield increases. During a wet year, we found that plant ET reached its potential so that reductions in actual plant ET dominated over increases in ground evaporation, resulting in a net increase in water yield. During a dry year, the relative dominance of these competing effects had greater spatial heterogeneity because the water stress status of the plants varied across the basin (as explained in Sect 4.2.2; Fig. 11).

However, the responses we observed in the dry year (1994) and in the wet year (1995) were also affected by the previous year's climate (mainly precipitation) and its effects on hydrologic and biogeochemical processes, which set the initial conditions for the dry and wet year (e.g., soil moisture, nitrogen availability, etc.). Therefore, we also analyzed other water years during the first ten years after beetle outbreak to examine whether our findings for dry and wet years follow a general pattern and to what extent they are influenced by antecedent conditions. Results indicate that our findings are robust throughout the study time period. For example, water yield generally decreased during dry years (1992, 1994, and 2001, see Figs. S1 and S2) and always increased during wet years (1993 and from 1995 to 2000, see Fig. S1 and S2).

Adams et al. (2012) provide a threshold of precipitation under which water yield increases after disturbances: at least 500 mm/year. The average annual precipitation over this study basin was 600-900 mm in dry years, and higher than 900 mm in wet years. Recent field observations also suggest that annual climate variability can affect the magnitude of evapotranspiration fluxes

567 that have potential to change the water yield direction (Biederman et al. 2014). Our results
568 corroborate these earlier studies by revealing that there are precipitation thresholds above which
569 tree removal increases water yield (Figs. 10, S1 and S2).

570 5.2 Role of vegetation mortality

571 Vegetation mortality is another important factor that influences water yield response. We
572 found that during the wet year, beetle outbreak increased water yield across the basin and the
573 magnitude of these increases grew linearly with the level of vegetation mortality (Fig. 10b). In
574 the dry year, however, the response of water yield to the level of vegetation mortality was more
575 complicated because mortality level influenced not only the magnitude of change but also the
576 direction (Fig. 10a). These opposing results (due to mortality level) mainly occurred in the
577 balanced northern part of the basin, where the competing effects of mortality (i.e., increases in
578 ground evaporation versus decreases in transpiration) are more balanced (Fig. 11). The level of
579 vegetation mortality played a less significant role in changing water yield in the southern "water-
580 limited" area. Vegetation mortality level determined the magnitudes of *Live LAI*, *Total LAI*,
581 transpiration, canopy evaporation, and ground evaporation in such a way that it governed the
582 direction of change in both ET and water yield. Thus, when vegetation mortality level was higher
583 than 40%, its effect of decreasing transpiration became the dominant process and its effect of
584 increasing soil evaporation became minor (Fig. 11 f and g; Guardiola-Claramonte et al. 2011).

585 Besides the precipitation threshold of at least 500 mm/year, Adams et al. (2012) also
586 estimate that when at least 20% of vegetation cover is removed, water yield can increase.
587 According to previous analysis (Sect 4.1), for a dry year, water yield increases when more than
588 40% of vegetation is removed (Fig. 10a). Our model simulations indicate similar mortality
589 thresholds exist for driving water yield increases during the dry year, however, we did not find

evidence that such a threshold exists during wet years. These differences between dry and wet years suggest that the effects of mortality on water yield depend on climate variability. Similarly, other studies demonstrate that the relationship between mortality level and water yield response is complicated and nonlinear (Moore and Wondzell 2005).

5.3 Role of long-term aridity index (PET/P)

Long-term aridity indices can be used to predict where water yield will decrease after disturbance. We found that water yield always increased in a wet year, irrespective of the climatic aridity index (Fig. 10a). For dry years, long-term aridity index was important in driving the direction of water yield responses to beetle outbreak. In areas that were less water-limited (balanced areas), the direction of water-yield responses to beetle outbreak in a dry year was mixed and depended on mortality level. For water-limited areas, in a dry year, water yield showed a more consistent decrease, and it was also less affected by mortality level. These results agree with previous studies finding that water yield decreases largely happen in semiarid areas (Guardiola-Claramonte et al. 2011; Biederman et al. 2014).

The decrease in water yield for water-limited area can be driven by increases in canopy evaporation or transpiration, which were different in the hydrologically-balanced area (driven by increase of ground evaporation). There, the increase in canopy evaporation was due to an increase in *Total LAI* which is a combined effect of delayed decay of dead foliage and fast growth of residual and understory plants (Fig. 11d type D5, D7, D8 & D9; Fig. S5). The surviving and understory plants in the water-limited also had higher transpiration rates after mortality (Fig. 11d type D6 and Fig. 8). Similarly, in field studies, Tsamir et al. (2019) found an increase in photosynthesis and transpiration after thinning in a semi-arid forest. These findings illustrate that in addition to top-down climate variability, the long-term aridity index (which also

613 varies with bottom-up drivers such as vegetation and local topography) can be another useful
614 indicator of how water yield will respond to disturbances.

615 In addition to evaporation and transpiration, snow sublimation can also influence the
616 direction of hydrologic responses. Similar to other process-based snow models, we found that
617 once dead foliage fell to the ground, canopy sublimation decreased (e.g., Sexstone et al. 2018;
618 Koeniger et al. 2008), which in turn increased water yield relative to the period when dead
619 needles remained on the trees (Fig. 5 and Fig. S7). In water-limited regions, the decrease in
620 canopy sublimation was much smaller than in the balanced regions because there were smaller
621 changes in *Total LAI* (Fig. S5 c and d). However, immediately after beetle outbreak (e.g., 1990 –
622 19992), we found that canopy sublimation increased in both regions due to an increase in *Total*
623 *LAI* (Fig. S7). This finding is supported by observational studies showing that canopy
624 sublimation can increase with increasing leaf area (Koeniger et al. 2008).

625 We also found that ground/snowpack sublimation decreased when all dead foliage fell to
626 the ground because snowmelt increased with the opening of the canopy. However, this finding
627 differs from other studies that suggest snowpack sublimation can increase with a more open
628 canopy (Biederman et al. 2014; Harpold et al. 2014). The latter can occur because open canopies
629 may allow more snow to reach ground, which can increase sublimation. However, in our study,
630 faster snowmelt appeared to dominate over increases in ground sublimation. These contrasts
631 between our research and previous studies illustrate a sophisticated balance between canopy-
632 atmosphere-environmental processes that must be accounted for when studying the sublimation
633 response to disturbances (Edburg et al. 2012; Frank et al. 2019). Although RHESSys is a
634 powerful tool for representing these complex interactions, some process representations warrant
635 further analysis. For example, RHESSys currently ignores the effects of litter on ground albedo

and snowmelt (Lundquist et al. 2013), which could affect Actual ET and PET rates, and therefore the long-term aridity index.

5.4 Uncertainties and recommendations for future research

We found the long-term (38-year) aridity index for our study region was a key driver influencing hydrologic responses to beetle outbreaks. While this trend is likely to continue in the future as climate change intensifies aridity in the western US (Livneh and Badger 2020), the classification of water-limited/balanced region based on 38-year aridity index may change. Thus, projecting how responses will change under future aridity scenarios requires further modeling research. We used historical 38-years (1980-2018) data to calculate the aridity index (PET/P). This method can be extended to project future responses to beetle outbreaks by using future climate data from generalized circulation models (GCMs) to drive the process-based, ecohydrologic-beetle effects model. Another consideration, however, is that as aridity continues to increase, vegetation may shift from evergreen to more drought-tolerant shrub or grass species. This would in turn alter beetle outbreak patterns and the corresponding water yield responses (Abatzoglou and Kolden 2013; Bart et al. 2016). However, this process is not well understood and is not currently represented in our modeling framework. A key uncertainty in predicting future beetle effects is how vegetation will respond to climate change.

Another key uncertainty is how beetle attacks will change in the future. We used uniform mortality levels for all patches across the watershed and focused our analyses on potential beetle effects. However, in reality beetles usually attack older trees first (Edburg et al. 2011). Thus, incorporating a more mechanistic understanding of beetle attack patterns with our beetle effects model could enable us to simulate more realistic outbreak scenarios moving forward. We also focused on water yield responses during the first 15 years after beetle outbreak in a watershed

659 that contained balanced or water-limited sub-basins. Future research should analyze long-term
660 effects (e.g., after the ecosystem begins to recover) on forest hydrology and also investigate
661 wetter, energy-limited regions.

662 **6 Conclusion**

663 We tested a coupled ecohydrologic and beetle effects model in a semi-arid basin in
664 southern Idaho to examine how watershed hydrology responds to beetle outbreak and how
665 interannual climatic variability, vegetation mortality, and long-term aridity influence these
666 responses. Simulation results indicate that each factor can play a discrete role in driving
667 hydrological processes (e.g., the direction and magnitude of changes in plant transpiration,
668 canopy and soil evaporation, soil and litter moisture, snow sublimation, etc.). These combined
669 effects determine the overall water budget and water yield of the basin. While interannual
670 climate variability is the key factor driving the direction of change in water yield, vegetation
671 mortality levels and long-term aridity modify water yield responses.

672 In dry years, the water yield of most sub-basins slightly decreased after beetle outbreak
673 when vegetation mortality was lower than 40%; while during wet years it increased in most sub-
674 basins. Our results show that long-term aridity index is a reliable indicator of the water yield
675 decreases that occur during dry years due to the fact that there is a consistent decrease in water
676 yield in the most water-limited portion of the basin. Generally, the effects of vegetation mortality
677 on water yield during dry years is less uniform and depends on local aridity. During wet years,
678 on the other hand, mortality typically causes increases in water yield. This illustrates that
679 together interannual climate variability and mortality can have a stronger effect on the direction
680 of water yield response in water-limited regions than interannual climate variability alone. Future
681 studies to predict water yield response to disturbance should consider the interactions of these

682 factors and capture the fluctuations of competing water fluxes and storage change that control
683 overall water budget and water yield.

684 Using our novel RHESSys-beetle effects modeling framework, we demonstrate that the
685 direction of hydrologic response is a function of multiple factors (e.g., interannual climate
686 variability, vegetation mortality level, and long-term aridity) and that these results do not
687 necessarily *conflict* with each other but are representative of different conditions. The
688 mechanisms behind these changes compete with each other resulting in a water yield increases or
689 decreases (Fig. 1). Contradictory findings in previous studies may result from differing mortality
690 levels, or differences in aridity because the emergent drivers that dominate water yield responses
691 differ. Disentangling these drivers is difficult or impossible using a purely empirical approach
692 where it can be challenging or cost-prohibitive to experiment under a broad range of controlled
693 conditions. Distributed process-based models on the other hand, provide a useful tool for
694 examining these dynamics.

695 This study can assist water supply stakeholders in risk management in beetle outbreak
696 locations. For example, during wet years, more attention might be focused on balanced areas,
697 i.e., wet regions, for flooding and erosion risks after beetle outbreaks since these regions may
698 experience large increase in runoff due to decreases in plant transpiration and increases in soil
699 moisture. During the dry years, attention might need to shift to "water-limited" areas for
700 managing wildfire risk since these regions will experience elevated ET and lower soil and litter
701 moisture. Because multiple factors interact to influence hydrological processes after beetle
702 outbreak, water and forests management must respond to spatial and temporal variations in
703 climate, aridity, and vegetation mortality levels.

704

Code and data availability

The coupled RHESSys model code is available online at:

https://github.com/renjianning/RHESSys/releases/tag/7.1.1

The data used in this study are available at:

https://osf.io/tsu9z/?view_only=72bfa7b376ad40c59278312f49b03a69

Author contributions

JR, JA and JAH conceived of study. JR designed study with support from JA, JAH and EH. JR and EH developed RHESSys code for coupling beetle effect model and parallelizing model runs with help from JA, JAH, NT, ML, CK, and JTA. JR performed model simulations and developed figures with help from all authors. ML and JTA generated downscaled meteorological data. JR wrote manuscript with input from all authors.

Competing interests

The authors declare that they have no conflict of interest.

Acknowledgments

This project is supported by National Science Foundation of United States under award numbers DMS-1520873 and DEB-1916658.

References

Abatzoglou, John T. 2013. "Development of Gridded Surface Meteorological Data for Ecological Applications and Modelling." *International Journal of Climatology* 33 (1): 121–31. https://doi.org/10.1002/joc.3413.

Abatzoglou, John T., and Crystal A. Kolden. 2011. "Climate Change in Western US Deserts: Potential for Increased Wildfire and Invasive Annual Grasses." Rangeland Ecology & Management 64 (5): 471–78. https://doi.org/10.2111/REM-D-09-00151.1

Ackerly, David D. 2004. "Adaptation, Niche Conservatism, and Convergence: Comparative Studies of Leaf Evolution in the California Chaparral." *The American Naturalist* 163 (5): 654–71. https://doi.org/10.1086/383062.

Adams, Henry D., Charles H. Luce, David D. Breshears, Craig D. Allen, Markus Weiler, V. Cody Hale, Alistair M. S. Smith, and Travis E. Huxman. 2012. "Ecohydrological Consequences of Drought- and Infestation- Triggered Tree Die-off: Insights and Hypotheses." *Ecohydrology* 5 (2): 145–59. https://doi.org/10.1002/eco.233.

Anderegg, William R. L., Jeffrey M. Kane, and Leander D. L. Anderegg. 2013. "Consequences of Widespread Tree Mortality Triggered by Drought and Temperature Stress." *Nature Climate Change* 3 (1): 30–36. https://doi.org/10.1038/nclimate1635.

Baret, F., A. Olioso, J. L. Luciani, J. F. Hanocq, and J. C. Monterrot. 1989. "Estimation à partir de mesures de réflectance spectrale du rayonnement photosynthétiquement actif absorbé par une culture de blé." *Agronomie* 9 (9): 885–95. https://doi.org/10.1051/agro:19890906.

Bart, Ryan R., Christina L. Tague, and Max A. Moritz. 2016. "Effect of Tree-to-Shrub Type Conversion in Lower Montane Forests of the Sierra Nevada (USA) on Streamflow." Edited by Julia A. Jones. *PLOS ONE* 11 (8): e0161805. https://doi.org/10.1371/journal.pone.0161805.

Bennett, Katrina E., Theodore J. Bohn, Kurt Solander, Nathan G. McDowell, Chonggang Xu, Enrique Vivoni, and Richard S. Middleton. 2018. "Climate-Driven Disturbances in the San Juan River Sub-Basin of the Colorado River." *Hydrology and Earth System Sciences* 22 (1): 709–25. https://doi.org/10.5194/hess-22-709-2018.

Bentz, Barbara J., Jacques Régnière, Christopher J Fettig, E. Matthew Hansen, Jane L. Hayes, Jeffrey A. Hicke, Rick G. Kelsey, Jose F. Negrón, and Steven J. Seybold. 2010. "Climate Change and Bark Beetles of the Western United States and Canada: Direct and Indirect Effects." *BioScience* 60 (8): 602–13. https://doi.org/10.1525/bio.2010.60.8.6.

BERNER, L. T., B. E. LAW, A. J. MEDDENS, and J. A. HICKE. 2017. "Tree Mortality from Fires and Bark Beetles at 1-Km Resolution, Western USA, 2003-2012." Collection. Tree Mortality from Fires and Bark Beetles at 1-Km Resolution, Western USA, 2003-2012. 2017. https://doi.org/10.3334/ornldaac/1512.

Berner, Logan T., and Beverly E. Law. 2016. "Plant Traits, Productivity, Biomass and Soil Properties from Forest Sites in the Pacific Northwest, 1999–2014." *Scientific Data* 3 (1): 1–14. https://doi.org/10.1038/sdata.2016.2.

Bethlahmy, Nedavia. 1974. "More Streamflow after a Bark Beetle Epidemic." *Journal of Hydrology* 23 (3): 185–89. https://doi.org/10.1016/0022-1694(74)90001-8.

Biederman, J. A., A. A. Harpold, D. J. Gochis, B. E. Ewers, D. E. Reed, S. A. Papuga, and P. D. Brooks. 2014. "Increased Evaporation Following Widespread Tree Mortality Limits Streamflow Response." *Water Resources Research* 50 (7): 5395–5409. https://doi.org/10.1002/2013WR014994.

767 Biederman, J. A., A. A. Harpold, D. J. Gochis, B. E. Ewers, D. E. Reed, S. A. Papuga, and P. D.
768 Brooks. 2014. “Increased Evaporation Following Widespread Tree Mortality Limits
769 Streamflow Response.” *Water Resources Research* 50 (7): 5395–5409.
770 https://doi.org/10.1002/2013WR014994.
771 Buhidar, Balthasar. 2002. “The Big Wood River Watershed Management Plan.”
772 https://www.deq.idaho.gov/media/450316-
773 _water_data_reports_surface_water_tmdls_big_wood_river_big_wood_entire.pdf.
774 Buma, Brian, and Ben Livneh. 2017. “Key Landscape and Biotic Indicators of Watersheds
775 Sensitivity to Forest Disturbance Identified Using Remote Sensing and Historical
776 Hydrography Data.” *Environmental Research Letters* 12 (7): 074028.
777 https://doi.org/10.1088/1748-9326/aa7091.
778 Chaney, Nathaniel W., Eric F. Wood, Alexander B. McBratney, Jonathan W. Hempel, Travis W.
779 Nauman, Colby W. Brungard, and Nathan P. Odgers. 2016. “POLARIS: A 30-Meter
780 Probabilistic Soil Series Map of the Contiguous United States.” *Geoderma* 274 (July):
781 54–67. https://doi.org/10.1016/j.geoderma.2016.03.025.
782 Chen, Fei, Guo Zhang, Michael Barlage, Ying Zhang, Jeffrey A. Hicke, Arjan Meddens,
783 Guangsheng Zhou, William J. Massman, and John Frank. 2014. “An Observational and
784 Modeling Study of Impacts of Bark Beetle–Caused Tree Mortality on Surface Energy and
785 Hydrological Cycles.” *Journal of Hydrometeorology* 16 (2): 744–61.
786 https://doi.org/10.1175/JHM-D-14-0059.1.
787 Daly, Christopher, Ronald P. Neilson, and Donald L. Phillips. 1994. “A Statistical-Topographic
788 Model for Mapping Climatological Precipitation over Mountainous Terrain.” *Journal of*
789 *Applied Meteorology* 33 (2): 140–58. https://doi.org/10.1175/1520-
790 0450(1994)033<0140:ASTMFM>2.0.CO;2.
791 Dickinson, Robert E., Muhammad Shaikh, Ross Bryant, and Lisa Graumlich. 1998. “Interactive
792 Canopies for a Climate Model.” *Journal of Climate* 11 (11): 2823–36.
793 https://doi.org/10.1175/1520-0442(1998)011<2823:ICFACM>2.0.CO;2.
794 Edburg, Steven L., Jeffrey A. Hicke, Paul D. Brooks, Elise G. Pendall, Brent E. Ewers, Urszula
795 Norton, David Gochis, Ethan D. Gutmann, and Arjan JH Meddens. 2012. “Cascading
796 Impacts of Bark Beetle-Caused Tree Mortality on Coupled Biogeophysical and
797 Biogeochemical Processes.” *Frontiers in Ecology and the Environment* 10 (8): 416–24.
798 https://doi.org/10.1890/110173.
799 Edburg, Steven L., Jeffrey A. Hicke, David M. Lawrence, and Peter E. Thornton. 2011.
800 “Simulating Coupled Carbon and Nitrogen Dynamics Following Mountain Pine Beetle
801 Outbreaks in the Western United States.” *Journal of Geophysical Research:*
802 *Biogeosciences* 116 (G4): G04033. https://doi.org/10.1029/2011JG001786.
803 Fan, Y., M. Clark, D. M. Lawrence, S. Swenson, L. E. Band, S. L. Brantley, P. D. Brooks, et al.
804 2019. “Hillslope Hydrology in Global Change Research and Earth System Modeling.”
805 *Water Resources Research* 0 (0). https://doi.org/10.1029/2018WR023903.
806 Farquhar, G. D., and S. von Caemmerer. 1982. “Modelling of Photosynthetic Response to
807 Environmental Conditions.” In *Physiological Plant Ecology II: Water Relations and*
808 *Carbon Assimilation*, edited by O. L. Lange, P. S. Nobel, C. B. Osmond, and H. Ziegler,
809 549–87. Encyclopedia of Plant Physiology. Berlin, Heidelberg: Springer.
810 https://doi.org/10.1007/978-3-642-68150-9_17.

811 Frank, John M., William J. Massman, Brent E. Ewers, and David G. Williams. 2019. “Bayesian
812 Analyses of 17 Winters of Water Vapor Fluxes Show Bark Beetles Reduce Sublimation.”
813 *Water Resources Research* 55 (2): 1598–1623. https://doi.org/10.1029/2018WR023054.
814 Frenzel, Steven A. 1989. “Water Resources of the Upper Big Wood River Basin, Idaho.” US
815 GEological Survey. https://idwr.idaho.gov/files/legal/CMR50/CMR50-1989-Water-
816 Resources-of-the-Upper-Big-Wood-River-Basin-Idaho.pdf.
817 Fyfe, John C., Chris Derksen, Lawrence Mudryk, Gregory M. Flato, Benjamin D. Santer, Neil C.
818 Swart, Noah P. Molotch, et al. 2017. “Large Near-Term Projected Snowpack Loss over
819 the Western United States.” *Nature Communications* 8 (1): 14996.
820 https://doi.org/10.1038/ncomms14996.
821 Garcia, E. S., and C. L. Tague. 2015. “Subsurface Storage Capacity Influences Climate–
822 Evapotranspiration Interactions in Three Western United States Catchments.” *Hydrology*
823 *and Earth System Sciences* 19 (12): 4845–58. https://doi.org/10.5194/hess-19-4845-2015.
824 Goeking, Sara A., and David G. Tarboton. 2020. “Forests and Water Yield: A Synthesis of
825 Disturbance Effects on Streamflow and Snowpack in Western Coniferous Forests.”
826 *Journal of Forestry* 118 (2): 172–92. https://doi.org/10.1093/jofore/fvz069.
827 Guardiola-Claramonte, M., Peter A. Troch, David D. Breshears, Travis E. Huxman, Matthew B.
828 Switanek, Matej Durcik, and Neil S. Cobb. 2011. “Decreased Streamflow in Semi-Arid
829 Basins Following Drought-Induced Tree Die-off: A Counter-Intuitive and Indirect
830 Climate Impact on Hydrology.” *Journal of Hydrology* 406 (3): 225–33.
831 https://doi.org/10.1016/j.jhydrol.2011.06.017.
832 Hanan, Erin J., Carla M. D’Antonio, Dar A. Roberts, and Joshua P. Schimel. 2016. “Factors
833 Regulating Nitrogen Retention During the Early Stages of Recovery from Fire in Coastal
834 Chaparral Ecosystems.” *Ecosystems* 19 (5): 910–26. https://doi.org/10.1007/s10021-016-
835 9975-0.
836 Hanan, Erin J., Christina Tague, Janet Choate, Mingliang Liu, Crystal Kolden, and Jennifer
837 Adam. 2018. “Accounting for Disturbance History in Models: Using Remote Sensing to
838 Constrain Carbon and Nitrogen Pool Spin-Up.” *Ecological Applications: A Publication*
839 *of the Ecological Society of America* 28 (5): 1197–1214.
840 https://doi.org/10.1002/eap.1718.
841 Hanan, Erin J., Christina (Naomi) Tague, and Joshua P. Schimel. 2017. “Nitrogen Cycling and
842 Export in California Chaparral: The Role of Climate in Shaping Ecosystem Responses to
843 Fire.” *Ecological Monographs* 87 (1): 76–90. https://doi.org/10.1002/ecm.1234.
844 Hanan, Erin J., Jianning Ren, Christina L. Tague, Crystal A. Kolden, John T. Abatzoglou, Ryan
845 R. Bart, Maureen C. Kennedy, Mingliang Liu, and Jennifer C. Adam. 2021. “How
846 Climate Change and Fire Exclusion Drive Wildfire Regimes at Actionable Scales.”
847 Environmental Research Letters 16 (2): 024051. https://doi.org/10.1088/1748-
848 9326/abd78e.
849 Harpold, Adrian A., Joel A. Biederman, Katherine Condon, Manuel Merino, Yoganand
850 Korgaonkar, Tongchao Nan, Lindsey L. Sloat, Morgan Ross, and Paul D. Brooks. 2014.
851 “Changes in Snow Accumulation and Ablation Following the Las Conchas Forest Fire,
852 New Mexico, USA: CHANGES IN SNOW FOLLOWING FIRE.” *Ecohydrology* 7 (2):
853 440–52. https://doi.org/10.1002/eco.1363.
854 Hicke, Jeffrey A., Morris C. Johnson, Jane L. Hayes, and Haiganoush K. Preisler. 2012. “Effects
855 of Bark Beetle-Caused Tree Mortality on Wildfire.” *Forest Ecology and Management*
856 271 (May): 81–90. https://doi.org/10.1016/j.foreco.2012.02.005.

857 Homer, Collin G., Jon Dewitz, Limin Yang, Suming Jin, Patrick Danielson, George Z. Xian,
858 John Coulston, Nathaniel Herold, James Wickham, and Kevin Megown. 2015.
859 "Completion of the 2011 National Land Cover Database for the Conterminous United
860 States – Representing a Decade of Land Cover Change Information." *Photogrammetric*
861 *Engineering and Remote Sensing* 81: 345354.
862 Hubbart, Jason A. 2007. "Timber Harvest Impacts on Water Yield in the Continental/Maritime
863 Hydroclimatic Region of the United States," 12.
864 Koeniger, Paul, Jason Hubbart, Timothy Link, and John Marshall. 2008. "Isotopic Variation of
865 Snowcover and Streamflow in Response to Changes in Canopy Structure in a Snow-
866 Dominated Mountain Catchment." *Hydrological Processes* 22 (February): 557–66.
867 Law, B. E., O. J. Sun, J. Campbell, S. Van Tuyl, and P. E. Thornton. 2003. "Changes in Carbon
868 Storage and Fluxes in a Chronosequence of Ponderosa Pine." *Global Change Biology* 9
869 (4): 510–24. https://doi.org/10.1046/j.1365-2486.2003.00624.x.
870 Lawrence, David M., Keith W. Oleson, Mark G. Flanner, Peter E. Thornton, Sean C. Swenson,
871 Peter J. Lawrence, Xubin Zeng, et al. 2011. "Parameterization Improvements and
872 Functional and Structural Advances in Version 4 of the Community Land Model."
873 *Journal of Advances in Modeling Earth Systems* 3 (1).
874 https://doi.org/10.1029/2011MS00045.
875 Lin, Laurence, Lawrence E. Band, James M. Vose, Taehee Hwang, Chelcy Ford Miniat, and
876 Paul V. Bolstad. 2019. "Ecosystem Processes at the Watershed Scale: Influence of
877 Flowpath Patterns of Canopy Ecophysiology on Emergent Catchment Water and Carbon
878 Cycling." *Ecohydrology* 0 (0): e2093. https://doi.org/10.1002/eco.2093.
879 Livneh, Ben, and Andrew M. Badger. 2020. "Drought Less Predictable under Declining Future
880 Snowpack." *Nature Climate Change* 10 (5): 452–58. https://doi.org/10.1038/s41558-020-
881 0754-8.
882 Livneh, Ben, Jeffrey S. Deems, Brian Buma, Joseph J. Barsugli, Dominik Schneider, Noah P.
883 Molotch, K. Wolter, and Carol A. Wessman. 2015. "Catchment Response to Bark Beetle
884 Outbreak and Dust-on-Snow in the Colorado Rocky Mountains." *Journal of Hydrology*
885 523 (April): 196–210. https://doi.org/10.1016/j.jhydrol.2015.01.039.
886 Lundquist, Jessica D., Susan E. Dickerson-Lange, James A. Lutz, and Nicoleta C. Cristea. 2013.
887 "Lower Forest Density Enhances Snow Retention in Regions with Warmer Winters: A
888 Global Framework Developed from Plot-Scale Observations and Modeling." *Water*
889 *Resources Research* 49 (10): 6356–70. https://doi.org/10.1002/wrcr.20504.
890 Lundquist, Jessica D., Paul J. Neiman, Brooks Martner, Allen B. White, Daniel J. Gottas, and F.
891 Martin Ralph. 2008. "Rain versus Snow in the Sierra Nevada, California: Comparing
892 Doppler Profiling Radar and Surface Observations of Melting Level." *Journal of*
893 *Hydrometeorology* 9 (2): 194–211. https://doi.org/10.1175/2007JHM853.1.
894 McVicar, Tim R., Michael L. Roderick, Randall J. Donohue, Ling Tao Li, Thomas G. Van Niel,
895 Axel Thomas, Jürgen Grieser, et al. 2012. "Global Review and Synthesis of Trends in
896 Observed Terrestrial Near-Surface Wind Speeds: Implications for Evaporation." *Journal*
897 *of Hydrology* 416–417 (January): 182–205. https://doi.org/10.1016/j.jhydrol.2011.10.024.
898 Meddens, Arjan, Jeffrey A Hicke, and Charles A Ferguson. 2012. "Spatiotemporal Patterns of
899 Observed Bark Beetle-Caused Tree Mortality in British Columbia and the Western
900 United States." *Ecological Applications : A Publication of the Ecological Society of*
901 *America* 22 (October): 1876–91. https://doi.org/10.2307/41723101.

902 Mikkelson, K. M., R. M. Maxwell, I. Ferguson, J. D. Stednick, J. E. McCray, and J. O. Sharp.
903 2013. “Mountain Pine Beetle Infestation Impacts: Modeling Water and Energy Budgets
904 at the Hill-Slope Scale.” *Ecohydrology* 6 (1): 64–72. https://doi.org/10.1002/eco.278.
905 Mitchell, Kenneth E., Dag Lohmann, Paul R. Houser, Eric F. Wood, John C. Schaake, Alan
906 Robock, Brian A. Cosgrove, et al. 2004. “The Multi-Institution North American Land
907 Data Assimilation System (NLDAS): Utilizing Multiple GCIP Products and Partners in a
908 Continental Distributed Hydrological Modeling System.” In .
909 https://doi.org/10.1029/2003JD003823.
910 Molotch, Noah P., Peter D. Blanken, Mark W. Williams, Andrew A. Turnipseed, Russell K.
911 Monson, and Steven A. Margulis. 2007. “Estimating Sublimation of Intercepted and Sub-
912 Canopy Snow Using Eddy Covariance Systems.” *Hydrological Processes* 21 (12): 1567–
913 75. https://doi.org/10.1002/hyp.6719.
914 Monteith, J. L. 1965. “Evaporation and Environment.” *Symposia of the Society for Experimental*
915 *Biology* 19: 205–34.
916 Montesi, James, Kelly Elder, R. A. Schmidt, and Robert E. Davis. 2004. “Sublimation of
917 Intercepted Snow within a Subalpine Forest Canopy at Two Elevations.” *Journal of*
918 *Hydrometeorology* 5 (5): 763–73. https://doi.org/10.1175/1525-
919 7541(2004)005<0763:SOISWA>2.0.CO;2.
920 Moore, R Dan, and S M Wondzell. 2005. “PHYSICAL HYDROLOGY AND THE EFFECTS
921 OF FOREST HARVESTING IN THE PACIFIC NORTHWEST: A REVIEW,” 22.
922 Morillas, L., R. E. Pangle, G. E. Maurer, W. T. Pockman, N. McDowell, C.-W. Huang, D. J.
923 Krofcheck, et al. 2017. “Tree Mortality Decreases Water Availability and Ecosystem
924 Resilience to Drought in Piñon-Juniper Woodlands in the Southwestern U.S.” *Journal of*
925 *Geophysical Research: Biogeosciences* 122 (12): 3343–61.
926 https://doi.org/10.1002/2017JG004095.
927 Mu, Qiaozhen, Faith Ann Heinsch, Maosheng Zhao, and Steven W. Running. 2007.
928 “Development of a Global Evapotranspiration Algorithm Based on MODIS and Global
929 Meteorology Data.” *Remote Sensing of Environment* 111 (4): 519–36.
930 https://doi.org/10.1016/j.rse.2007.04.015.
931 Mu, Qiaozhen, Maosheng Zhao, and Steven W. Running. 2011. “Improvements to a MODIS
932 Global Terrestrial Evapotranspiration Algorithm.” *Remote Sensing of Environment* 115
933 (8): 1781–1800. https://doi.org/10.1016/j.rse.2011.02.019.
934 Nash, J. E., and J. V. Sutcliffe. 1970. “River Flow Forecasting through Conceptual Models Part I
935 — A Discussion of Principles.” *Journal of Hydrology* 10 (3): 282–90.
936 https://doi.org/10.1016/0022-1694(70)90255-6.
937 NRCS. n.d. “SNOTEL.” https://www.wcc.nrcs.usda.gov/about/mon_automate.html.
938 Nagler, Pamela L., Uyen Nguyen, Heather L. Bateman, Christopher J. Jarchow, Edward P.
939 Glenn, William J. Waugh, and Charles van Riper. 2018. “Northern Tamarisk Beetle
940 (Diorhabda Carinulata) and Tamarisk (Tamarix Spp.) Interactions in the Colorado River
941 Basin.” *Restoration Ecology* 26 (2): 348–59. https://doi.org/10.1111/rec.12575.
942 Paine, T. D., K. F. Raffa, and T. C. Harrington. 1997. “Interactions Among Scolytid Bark
943 Beetles, Their Associated Fungi, and Live Host Conifers.” *Annual Review of Entomology*
944 42 (1): 179–206. https://doi.org/10.1146/annurev.ento.42.1.179.
945 Parton, W. J., A. R. Mosier, D. S. Ojima, D. W. Valentine, D. S. Schimel, K. Weier, and A. E.
946 Kulmala. 1996. “Generalized Model for N2 and N2O Production from Nitrification and

947 Denitrification." *Global Biogeochemical Cycles* 10 (3): 401–12.
948 https://doi.org/10.1029/96GB01455.
949 Penn, Colin A., Lindsay A. Bearup, Reed M. Maxwell, and David W. Clow. 2016. "Numerical
950 Experiments to Explain Multiscale Hydrological Responses to Mountain Pine Beetle Tree
951 Mortality in a Headwater Watershed." *Water Resources Research* 52 (4): 3143–61.
952 https://doi.org/10.1002/2015WR018300.
953 Perry, Timothy D., and Julia A. Jones. 2017. "Summer Streamflow Deficits from Regenerating
954 Douglas-Fir Forest in the Pacific Northwest, USA: Summer Streamflow Deficits from
955 Regenerating Douglas-Fir Forest." *Ecohydrology* 10 (2): e1790.
956 https://doi.org/10.1002/eco.1790.
957 Pomeroy, John, Xing Fang, and Chad Ellis. 2012. "Sensitivity of Snowmelt Hydrology in
958 Marmot Creek, Alberta, to Forest Cover Disturbance: SENSITIVITY OF SNOWMELT
959 HYDROLOGY TO FOREST DISTURBANCE." *Hydrological Processes* 26 (12): 1891–
960 1904. https://doi.org/10.1002/hyp.9248.
961 Potts, Donald F. 1984. "Hydrologic Impacts of a Large-Scale Mountain Pine Beetle
962 (Dendroctonus Ponderosae Hopkins) Epidemic1." *JAWRA Journal of the American*
963 *Water Resources Association* 20 (3): 373–77. https://doi.org/10.1111/j.1752-
964 1688.1984.tb04719.x.
965 Robles, Marcos D., Robert M. Marshall, Frances O'Donnell, Edward B. Smith, Jeanmarie A.
966 Haney, and David F. Gori. 2014. "Effects of Climate Variability and Accelerated Forest
967 Thinning on Watershed-Scale Runoff in Southwestern USA Ponderosa Pine Forests."
968 *PLOS ONE* 9 (10): e111092. https://doi.org/10.1371/journal.pone.0111092.
969 Ryan, Michael G. 1991. "Effects of Climate Change on Plant Respiration." *Ecological*
970 *Applications* 1 (2): 157–67. https://doi.org/10.2307/1941808.
971 Searcy, James Kincheon. 1959. "Flow-Duration Curves." Report 1542A. Water Supply Paper.
972 USGS Publications Warehouse. https://doi.org/10.3133/wsp1542A.
973 Sexstone, Graham A., David W. Clow, Steven R. Fassnacht, Glen E. Liston, Christopher A.
974 Hiemstra, John F. Knowles, and Colin A. Penn. 2018. "Snow Sublimation in Mountain
975 Environments and Its Sensitivity to Forest Disturbance and Climate Warming." *Water*
976 *Resources Research* 54 (2): 1191–1211. https://doi.org/10.1002/2017WR021172.
977 Skinner, Kenneth D. 2013. "Post-Fire Debris-Flow Hazard Assessment of the Area Burned by
978 the 2013 Beaver Creek Fire near Hailey, Central Idaho." USGS Numbered Series 2013–
979 1273. Open-File Report. Reston, VA: U.S. Geological Survey.
980 http://pubs.er.usgs.gov/publication/ofr20131273.
981 Slinski, Kimberly M., Terri S. Hogue, Aaron T. Porter, and John E. McCray. 2016. "Recent Bark
982 Beetle Outbreaks Have Little Impact on Streamflow in the Western United States."
983 *Environmental Research Letters* 11 (7): 074010. https://doi.org/10.1088/1748-
984 9326/11/7/074010.
985 Smith, Frederick W., D. Arthur Sampson, and James N. Long. 1991. "Comparison of Leaf Area
986 Index Estimates from Tree Allometrics and Measured Light Interception." *Forest Science*
987 37 (6): 1682–88. https://doi.org/10.1093/forestscience/37.6.1682.
988 Smith, Rex Onis. 1960. "Geohydrologic Evaluation of Streamflow Records in the Big Wood
989 River Basin, Idaho." USGS Numbered Series 1479. Water Supply Paper. U.S. Govt.
990 Print. Off.,. http://pubs.er.usgs.gov/publication/wsp1479.

Son, Kyongho, and Christina Tague. 2019. “Hydrologic Responses to Climate Warming for a Snow-Dominated Watershed and a Transient Snow Watershed in the California Sierra.” *Ecohydrology* 12 (1): e2053. https://doi.org/10.1002/eco.2053.

Sun, Ning, Mark Wigmosta, Tian Zhou, Jessica Lundquist, Susan Dickerson-Lange, and Nicoleta Cristea. 2018. “Evaluating the Functionality and Streamflow Impacts of Explicitly Modelling Forest–Snow Interactions and Canopy Gaps in a Distributed Hydrologic Model.” *Hydrological Processes* 32 (13): 2128–40. https://doi.org/10.1002/hyp.13150.

Snyder, Keirith A., Russell L. Scott, and Kenneth McGwire. 2012. “Multiple Year Effects of a Biological Control Agent (Diorhabda Carinulata) on Tamarix (Saltcedar) Ecosystem Exchanges of Carbon Dioxide and Water.” *Agricultural and Forest Meteorology* 164 (October): 161–69. https://doi.org/10.1016/j.agrformet.2012.03.004.

Tague, C. L., and L. E. Band. 2004. “RHESSys: Regional Hydro-Ecologic Simulation System—An Object-Oriented Approach to Spatially Distributed Modeling of Carbon, Water, and Nutrient Cycling.” *Earth Interactions* 8 (19): 1–42. https://doi.org/10.1175/1087-3562(2004)8<1:RRHSSO>2.0.CO;2.

Tague, Christina L., Max Moritz, and Erin Hanan. 2019. “The Changing Water Cycle: The Eco-Hydrologic Impacts of Forest Density Reduction in Mediterranean (Seasonally Dry) Regions.” *Wiley Interdisciplinary Reviews: Water* 0 (0): e1350. https://doi.org/10.1002/wat2.1350.

Tsamir, Mor, Sagi Gottlieb, Yakir Preisler, Eyal Rotenberg, Fyodor Tatarinov, Dan Yakir, Christina Tague, and Tamir Klein. 2019. “Stand Density Effects on Carbon and Water Fluxes in a Semi-Arid Forest, from Leaf to Stand-Scale.” *Forest Ecology and Management* 453 (December): 117573. https://doi.org/10.1016/j.foreco.2019.117573.

White, Joseph D., and Steven W. Running. 1994. “Testing Scale Dependent Assumptions in Regional Ecosystem Simulations.” *Journal of Vegetation Science* 5 (5): 687–702. https://doi.org/10.2307/3235883.

White, Michael A., Peter E. Thornton, Steven W. Running, and Ramakrishna R. Nemani. 2000. “Parameterization and Sensitivity Analysis of the BIOME–BGC Terrestrial Ecosystem Model: Net Primary Production Controls.” *Earth Interactions* 4 (3): 1–85. https://doi.org/10.1175/1087-3562(2000)004<0003:PASAOT>2.0.CO;2.

Wine, Michael L, Daniel Cadol, and Oleg Makhnin. 2018. “In Ecoregions across Western USA Streamflow Increases during Post-Wildfire Recovery.” *Environmental Research Letters* 13 (1): 014010. https://doi.org/10.1088/1748-9326/aa9c5a.

Winkler, Rita, Sarah Boon, Barbara Zimonick, and Dave Spittlehouse. 2014. “Snow Accumulation and Ablation Response to Changes in Forest Structure and Snow Surface Albedo after Attack by Mountain Pine Beetle.” *Hydrological Processes* 28 (2): 197–209. https://doi.org/10.1002/hyp.9574.

Zhang, Ke, John S. Kimball, Qiaozhen Mu, Lucas A. Jones, Scott J. Goetz, and Steven W. Running. 2009. “Satellite Based Analysis of Northern ET Trends and Associated Changes in the Regional Water Balance from 1983 to 2005.” *Journal of Hydrology* 379 (1): 92–110. https://doi.org/10.1016/j.jhydrol.2009.09.047.

Zhao, Maosheng, Steven W. Running, and Ramakrishna R. Nemani. 2006. “Sensitivity of Moderate Resolution Imaging Spectroradiometer (MODIS) Terrestrial Primary Production to the Accuracy of Meteorological Reanalyses.” *Journal of Geophysical Research: Biogeosciences* 111 (G1). https://doi.org/10.1029/2004JG000004.

Table 1. Classification of aridity index.

Aridity Index (i.e. PET/P)	Type
> 2	Water - limited
0.8 - 2	Balanced
< 0.8	Energy - limited

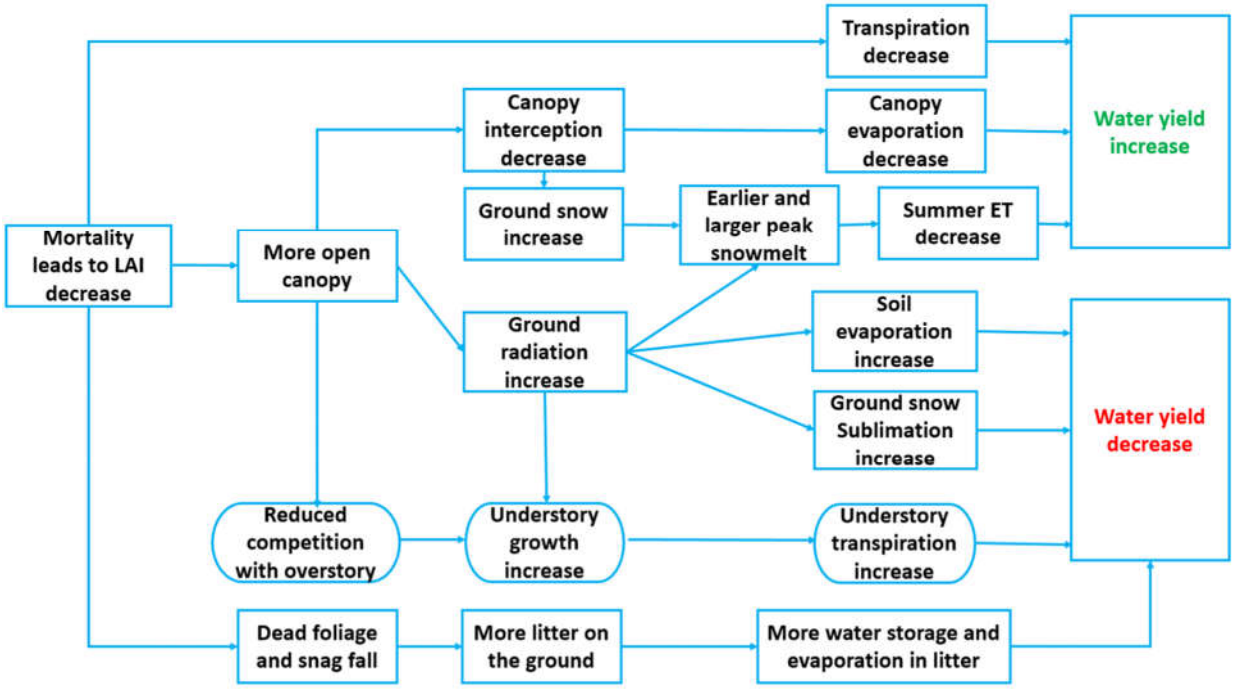

1043

1044 *Figure 1. Mechanism of water yield responses to beetle-caused mortality during the red and*
1045 *gray phases (0 – 10 years after beetle outbreak), semicircle boxes represent understory*
1046 *responses and square boxes represent overstory responses.*

1047

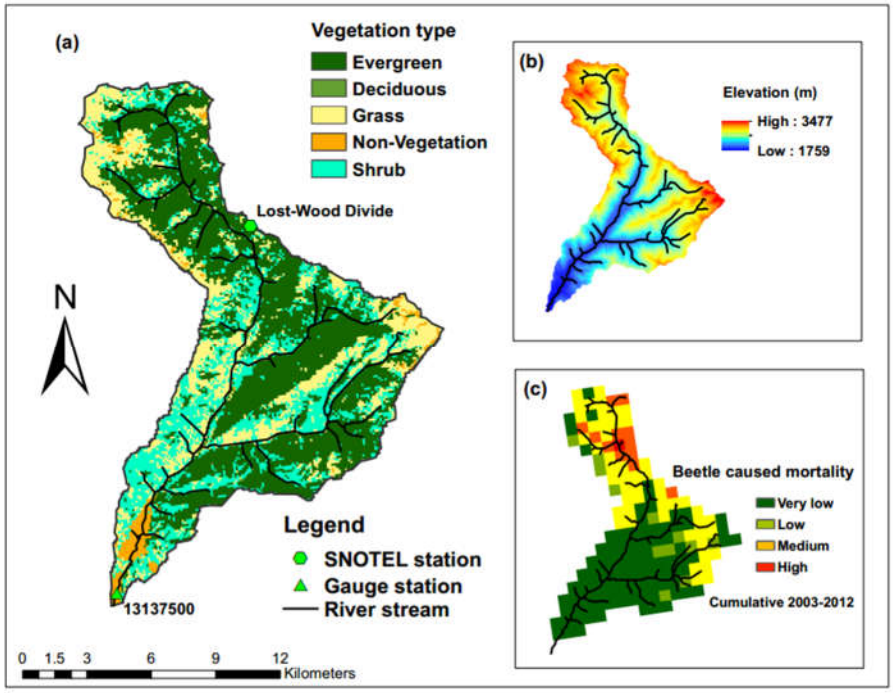

1048

1049 *Figure 2. Land cover, elevation, and tree mortality for Trail Creek. (a) is the land cover map*
1050 *with the main vegetation type, (b) is the elevation gradient, and (c) is the severity of beetle*
1051 *caused tree mortality (during the period 2003-2012 Meddens et al. (2012)). Note that, for our*
1052 *modeling experiments, we prescribe beetle outbreak uniformly across evergreen patches instead*
1053 *of using historical beetle outbreak data.*

1054

1055

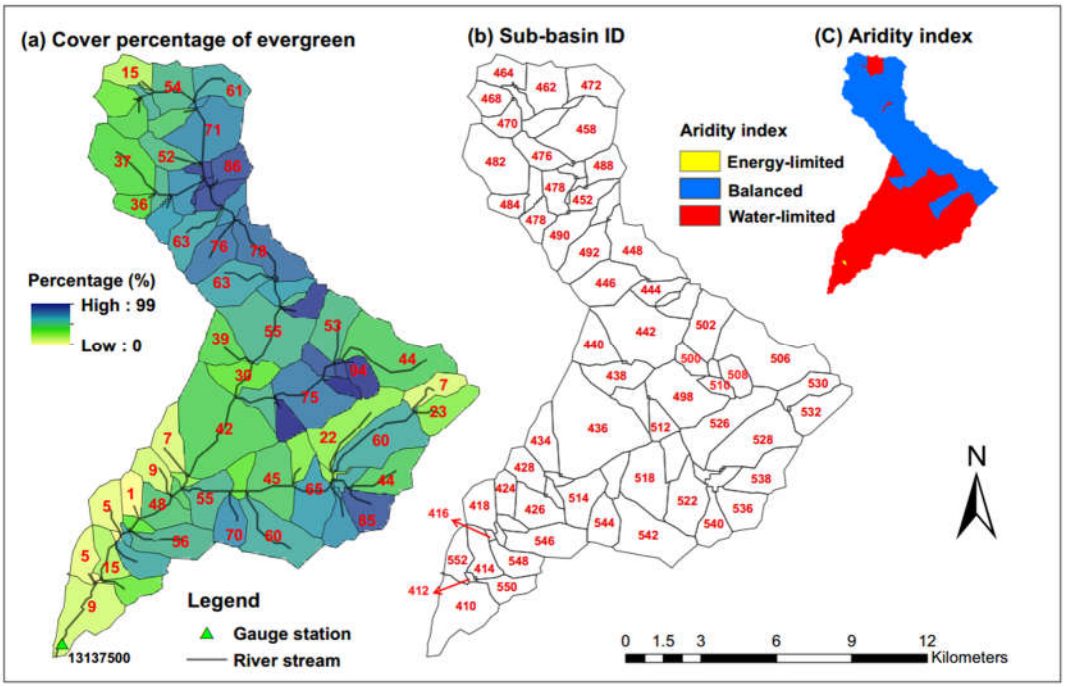

1056

1057 *Figure 3. Trail creek evergreen forest cover percentage for each sub-basin, sub-basin ID, and*
1058 *long-term aridity index. Aridity index is defined as annual mean potential evapotranspiration*
1059 *(PET) / precipitation (P) from 38 years of data (see Sect 3.4), PET/P > 2 is water-limited, PET/P*
1060 *< 0.8 is energy-limited, PET/P between 0.8 and 2 is balanced. Recall that only evergreen forest*
1061 *trees are attacked during beetle outbreaks.*
1062

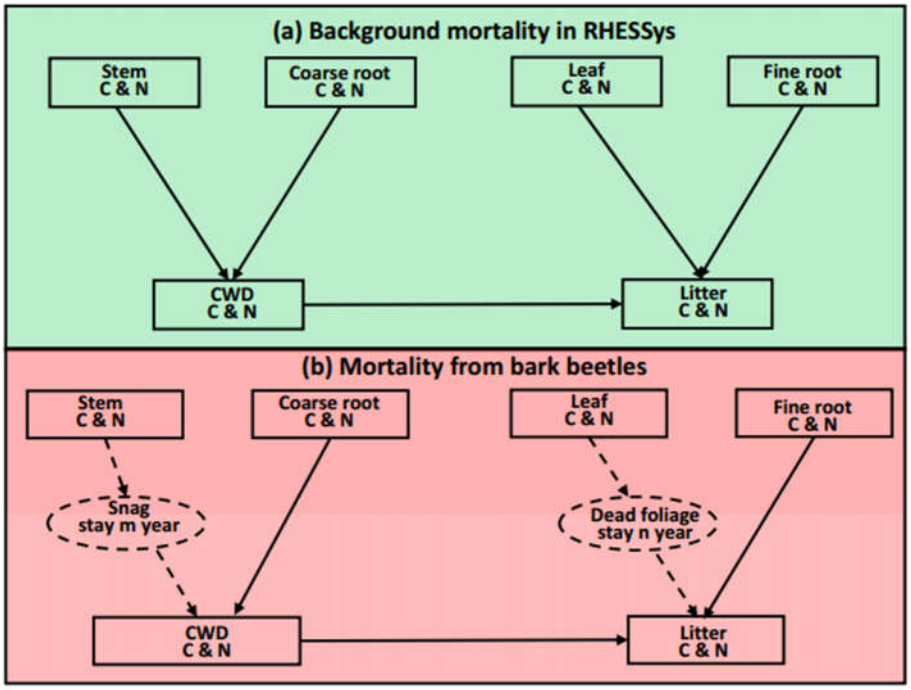

Figure 4. Conceptual framework of the beetle effect model. ***(a)*** *Normal background mortality routine in RHESSys before beetle outbreak.* ***(b)*** *Mortality from bark beetles. We add snag (standing dead trees) and dead foliage (needles still on dead trees) pools, shown in the dashed circle. After a beetle outbreak, carbon (C) and Nitrogen (N) move from stems to snag pools (black dashed arrow). After staying in the snag pool for m years, C and N move from snag to coarse wood debris pools (CWD) with an exponential decay rate to represent the snag fall (gray dashed arrow). It is a similar process for leaf C and N, which move from leaf to dead foliage to litter pools (black dotted arrow). Furthermore, C and N in the CWD and fine root pools move to the litter pool immediately after outbreak (solid black and gray arrows). Figure modified from Edburg et al. (2012).*

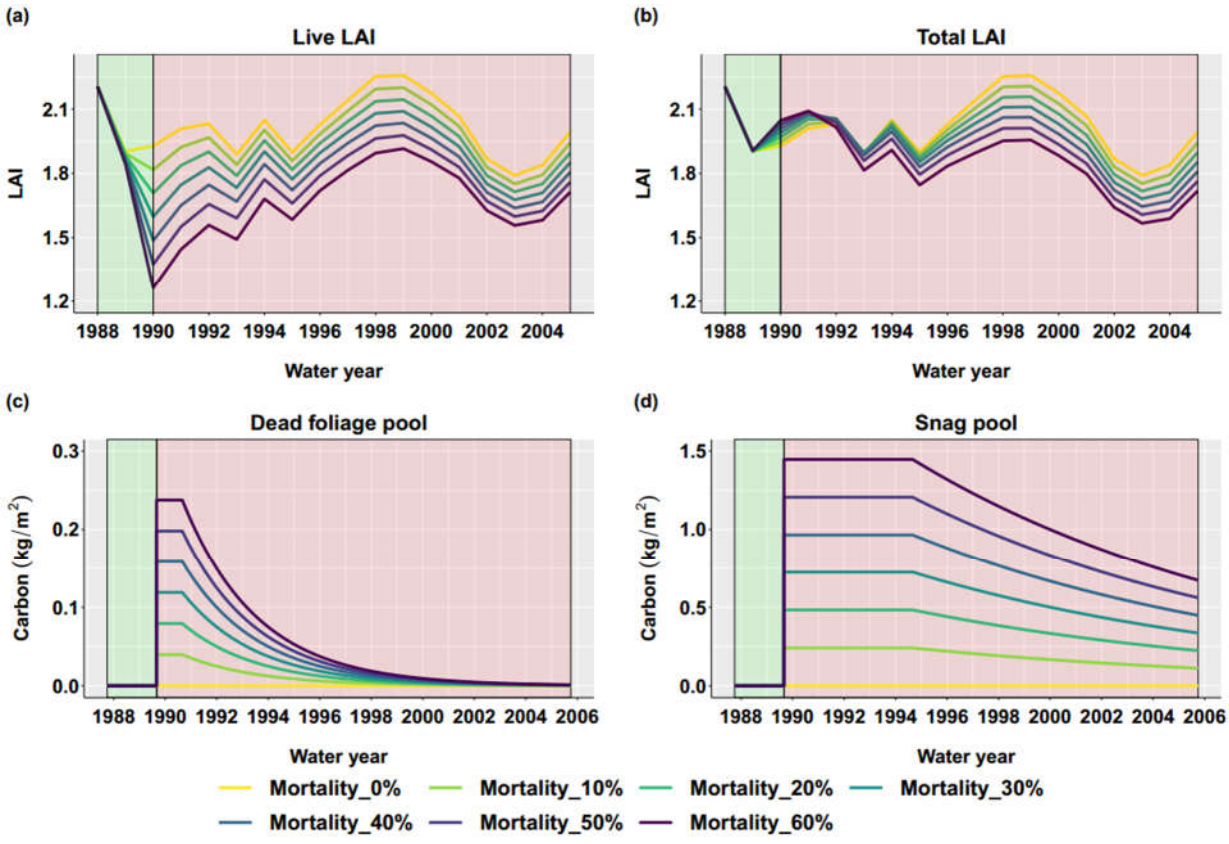

Figure 5. Basin-scale vegetation responses after beetle outbreak for different evergreen mortality level. (a) Annual live leaf area index (Live LAI), (b) Annual Total LAI (LAI calculated including dead foliage pool), (c) Daily dead foliage pool, and (d) Daily snag pool after outbreak. The green background color is the period before beetle outbreak, and the red background color is after the beetle outbreak.

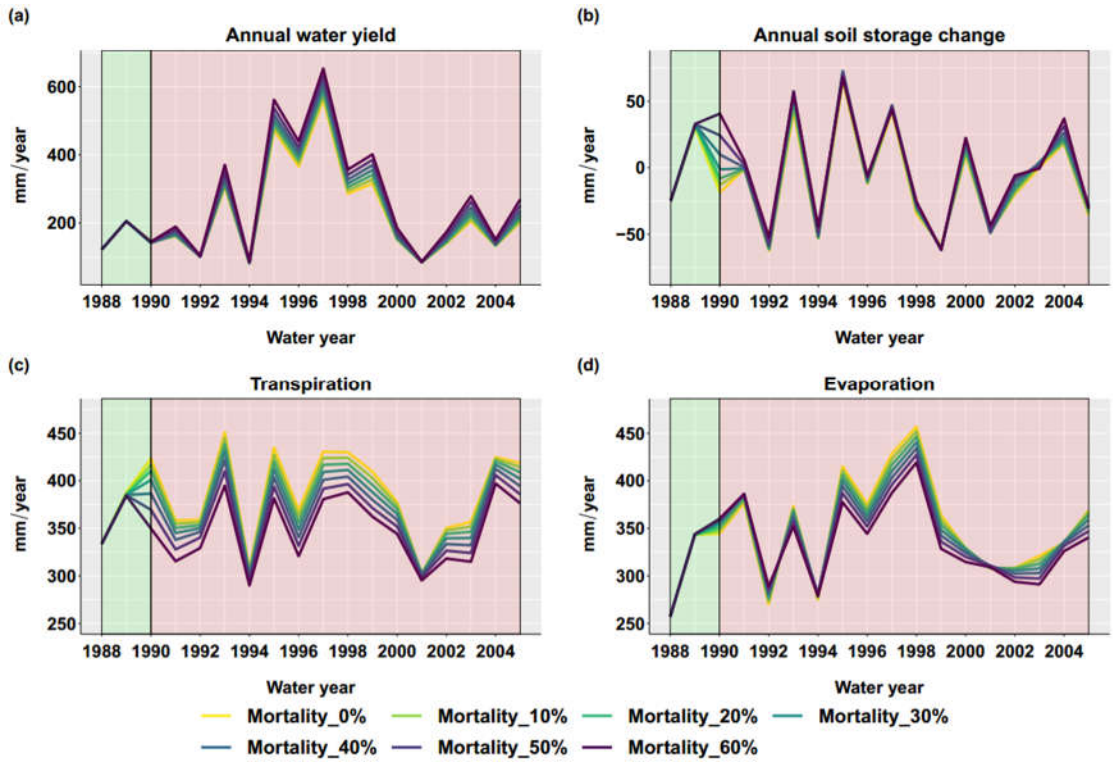

Figure 6. Basin-scale annual sum of hydrologic fluxes responses after beetle outbreak (1989) for different evergreen mortality levels. (a) Annual water yield calculated as annual sum of basin streamflow, and (b) annual soil water storage change calculated as water year soil water storage at the end of water year minus soil water storage at the beginning of water year. (c) Transpiration is the annual sum of transpiration for both overstory and understory. (d) Evaporation is calculated as the annual sum of canopy evaporation, ground evaporation, and snow sublimation.

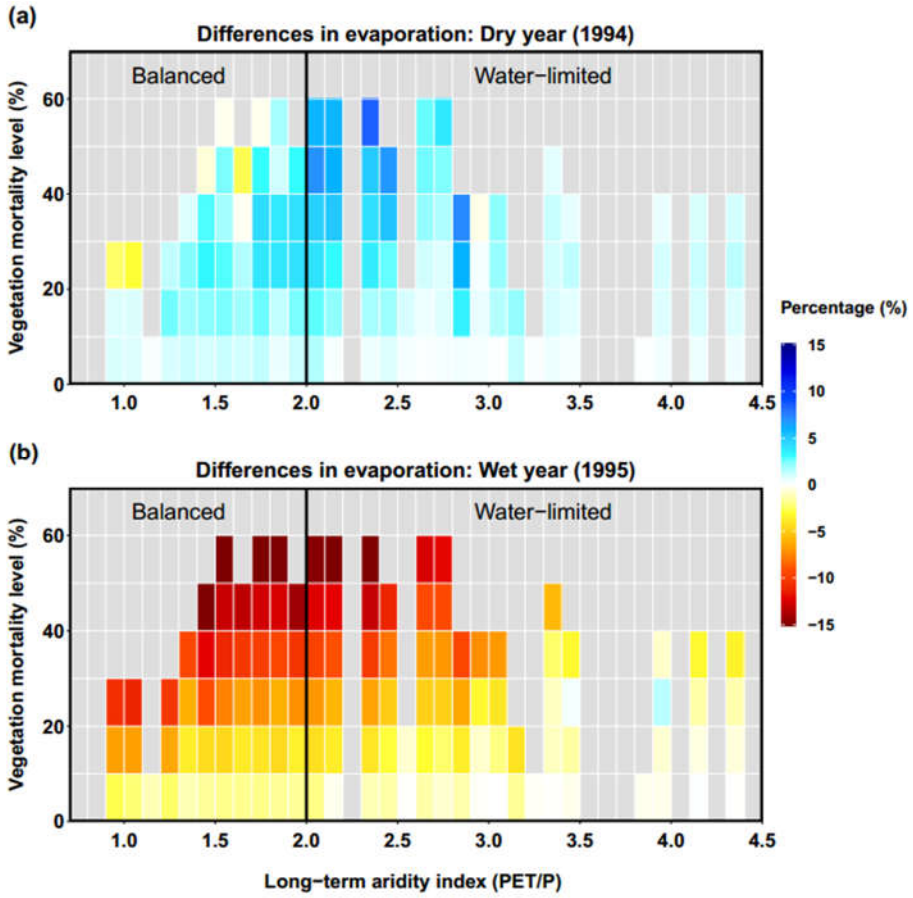

Figure 7. Relationship among long-term aridity, vegetation mortality level, and differences in evaporation for a dry year (1994, a) and wet year (1995, b). Differences are calculated as the normalized differences (%) of evaporation between each evergreen mortality scenario and the control run for no beetle outbreak. Vegetation mortality for each sub-basin is calculated as the percentage of evergreen patches multiplied by the mortality level of evergreen caused by beetles. Long-term aridity is defined as temporally averaged (38 years) potential evapotranspiration relative to precipitation.

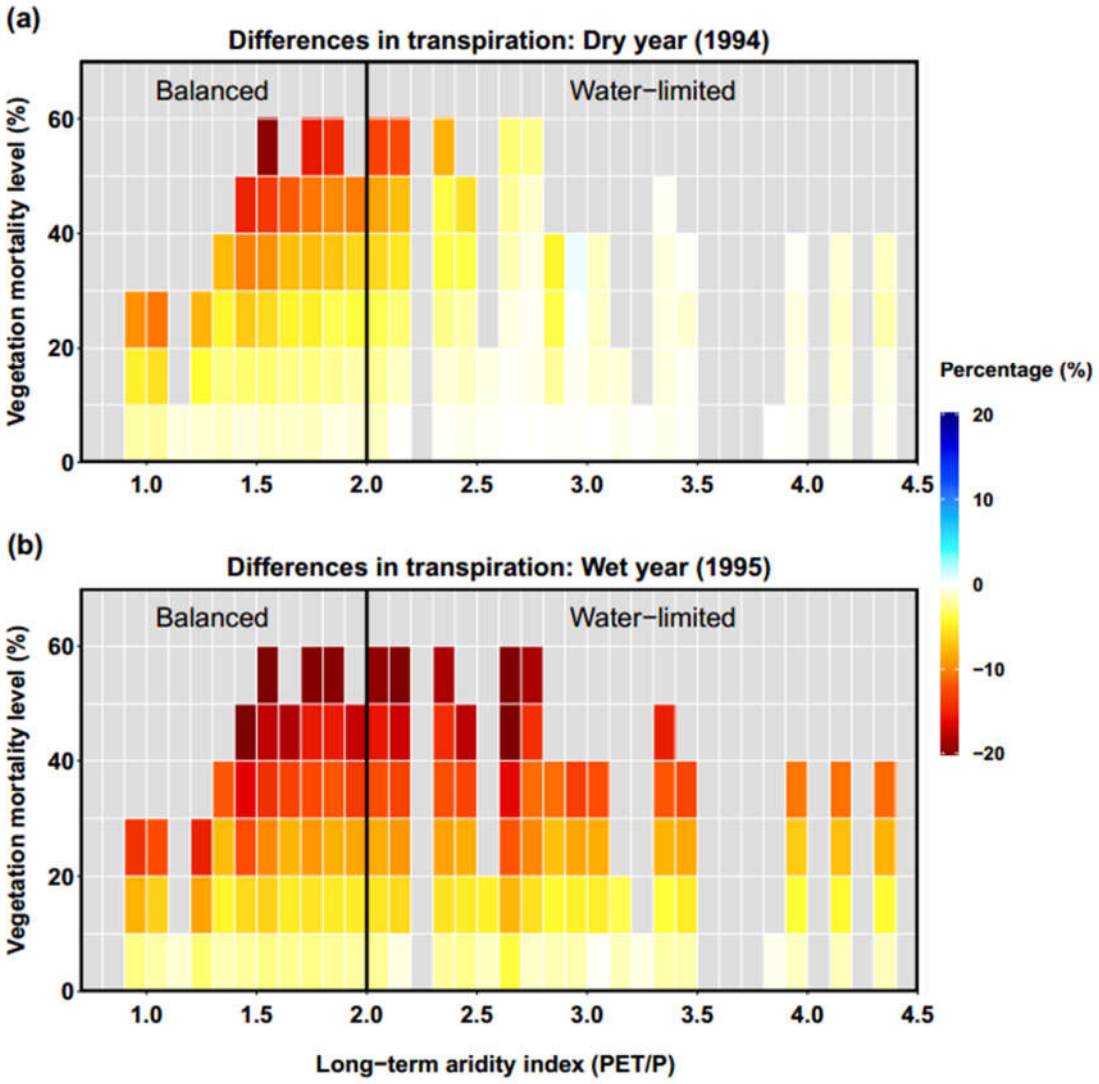

Figure 8. Relationship among long-term aridity, vegetation mortality, and differences in transpiration for a dry year (1994, a) and wet year (1995, b).

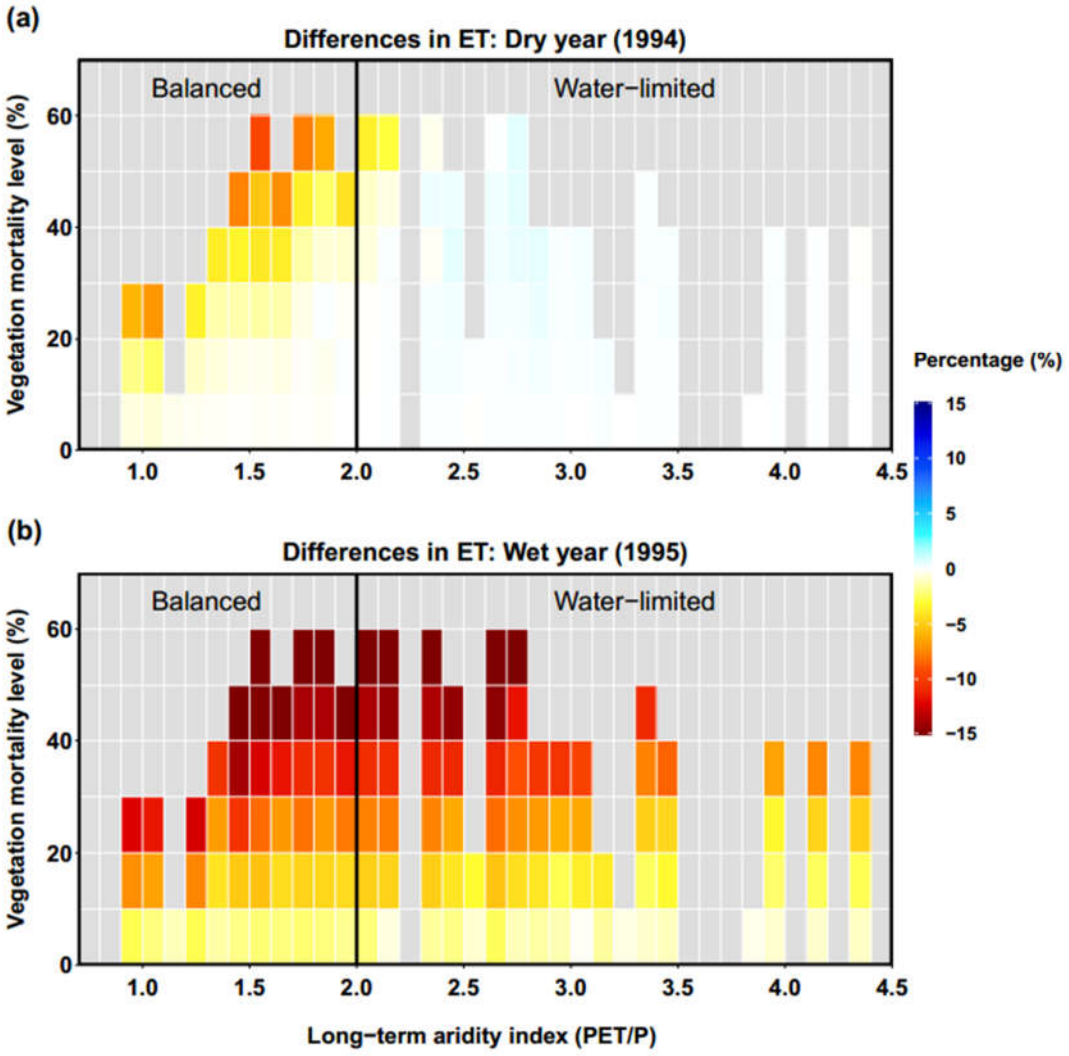

Figure 9. Relationship among long-term aridity, vegetation mortality level and differences in ET for a dry year (1994, a) and a wet year (1995, b).

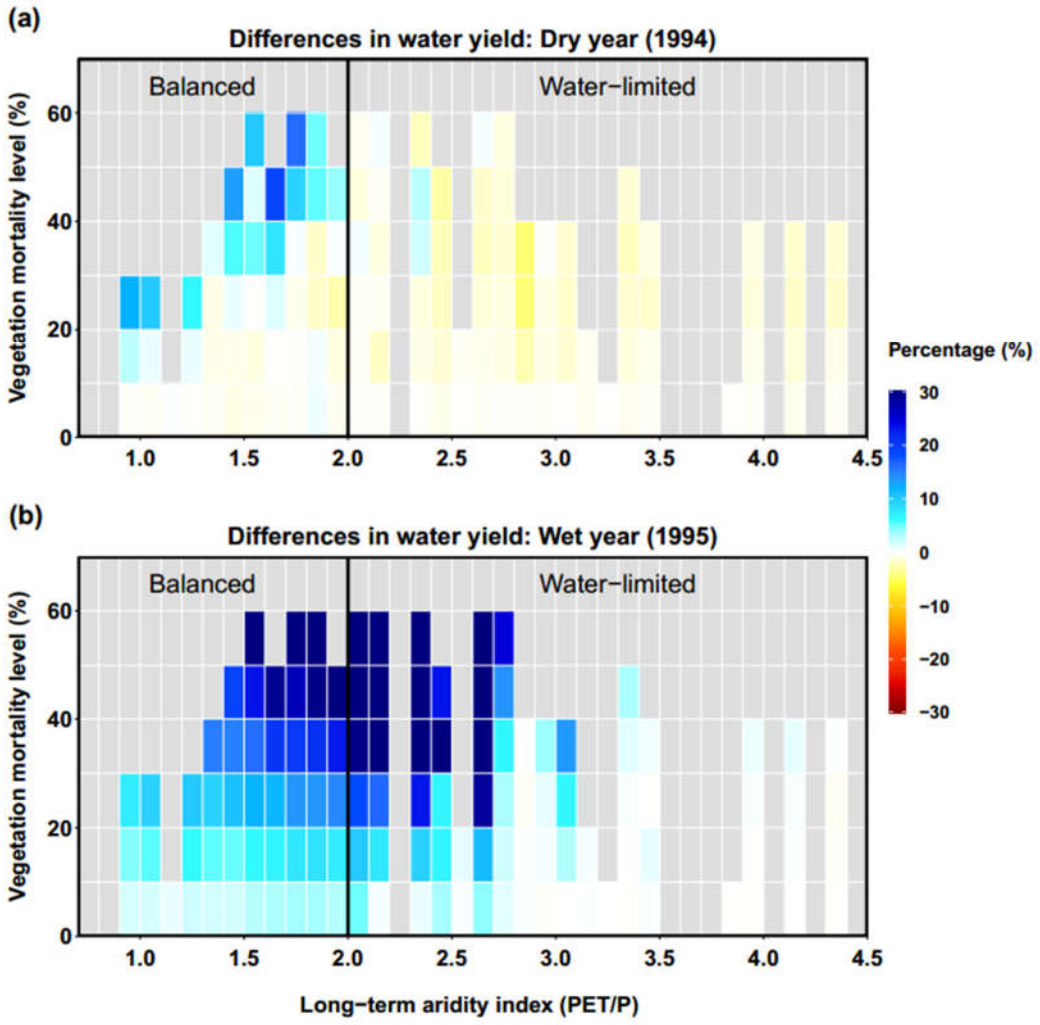

1108

1109 *Figure 10. Relationship among long-term aridity, vegetation mortality level and Differences in*
1110 *water yield for a dry year (1994, a) and wet year (1995, b).*
1111

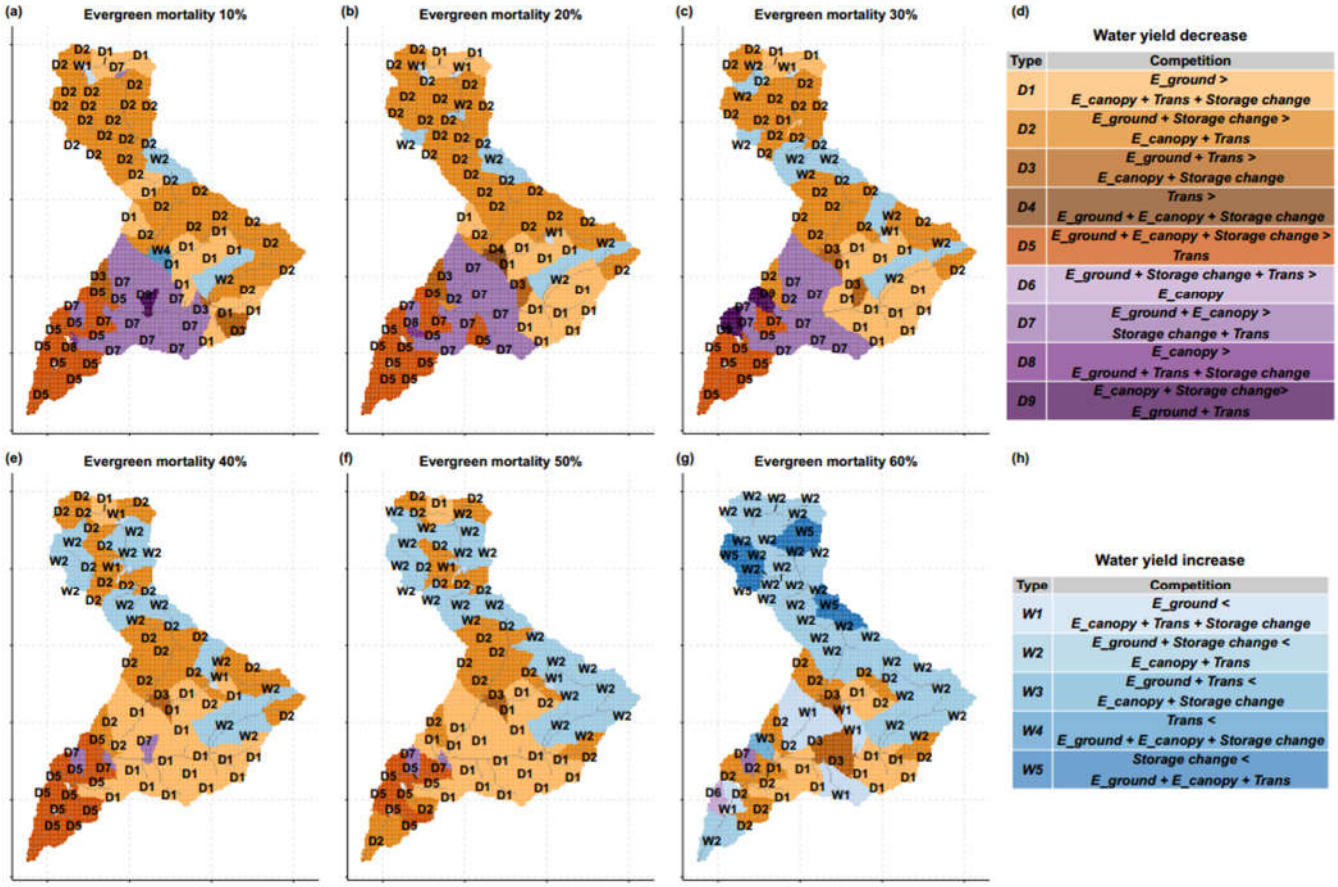

Figure 11. Water yield response types after beetle outbreak for different evergreen mortality scenarios compared with control scenario. D1 to D9 are water yield decrease types and W1 to W5 are water yield increase types. In panel D and H, the left side of each type are increasing fluxes that cause water yield decreases and the right side are decreasing fluxes that cause water yield increase. If the left side is larger than the right side, water yield increases, and vice versa. (Note: this mortality is evergreen mortality, which is different from vegetation mortality.)